European Journal of Pharmaceutical Sciences 120 (2018) 107–122

Contents lists available at ScienceDirect

European Journal of Pharmaceutical Sciences

journal homepage: www.elsevier.com/locate/ejps

Multi-kinetic release of benznidazole-loaded multiparticulate drug delivery systems based on polymethacrylate interpolyelectrolyte complexes

Mónica C. García[a,b], Marisa Martinelli[c], Nicolás E. Ponce[d], Liliana M. Sanmarco[e,f], María P. Aoki[e,f], Rubén H. Manzo[a,b], Alvaro F. Jimenez-Kairuz[a,b,*]

[a] Departamento de Ciencias Farmacéuticas, Facultad de Ciencias Químicas, Universidad Nacional de Córdoba, Córdoba, Argentina
[b] Unidad de Investigación y Desarrollo en Tecnología Farmacéutica – UNITEFA (CONICET-UNC), Córdoba, Argentina
[c] Instituto de Investigación y Desarrollo en Ingeniería de Procesos y Química Aplicada (IPQA), CONICET and Laboratorio de Materiales Poliméricos (LAMAP), Departamento de Química Orgánica, Facultad de Ciencias Químicas, Universidad Nacional de Córdoba, Ciudad Universitaria, X5000HUA Córdoba, Argentina
[d] Instituto de Investigación Médica "M. y M. Ferreyra", INIMEC-CONICET, Universidad Nacional de Córdoba, Córdoba, Argentina
[e] Centro de Investigaciones en Bioquímica Clínica e Inmunología CIBICI (CONICET-UNC), Córdoba, Argentina
[f] Departamento de Bioquímica Clínica, Facultad de Ciencias Químicas, Universidad Nacional de Córdoba, Córdoba, Argentina

ARTICLE INFO

Keywords:
Benznidazole
Eudragit®
Polyelectrolyte complexes
Multiparticulate drug delivery systems
Chagas disease

ABSTRACT

Interpolyelectrolyte complexes (IPEC) formulated as multiparticulate drug delivery systems (MDDS) are interesting carriers to improve drug' performance. Benznidazole (BZ) is the first–line drug for Chagas treatment; however, it presents side effects and toxicity, conditioning its efficacy and safety. The goal of this work was to obtain novel MDDS composed by IPEC based on different polymethacrylate carriers loaded with BZ and to investigate *in vitro* drug delivery performance for oral administration. Physicochemical characterizations were studied and preclinical studies in a murine model of acute Chagas disease were also performed. The MDDS composed by BZ-loaded IPEC based on polymethacrylates were obtained by casting solvent followed by wet granulation methods with yields > 83%. FT-IR demonstrated ionic interaction between the polyelectrolytes. Confocal microscopy, DSC and PXRD revealed a fraction uniformly distributed of free BZ on the multiparticles. The rheological evaluation of the MDDS showed adequate flow features for their formulation in hard gelatin-capsules. The type and composition of IPEC conditioned the modulation of BZ release and fluid uptake results. MDDS based on more hydrophylic Eudragit® showed very fast dissolution (Q_{15min} > 85%), while an extended release (Q_{120min} ≤ 40%) for the hydrophobic ones was observed. Capsules containing a combination of two MDDS with different release profile of BZ showed promising properties to improve Chagas disease pharmacotherapy in the preliminary *in vivo* assay performed, in which the BZ-loaded MDDS exhibited efficacy to reduce parasitemia, while decreasing the levels of liver injury markers in comparison to BZ conventional treatment. Multi-kinetic BZ delivery systems developed are interesting pharmaceutical alternatives to improve the treatment of Chagas disease.

1. Introduction

Chagas disease is caused by *Trypanosoma cruzi* infection and represents one of the most significant public health problems in Latin America due to its prevalence, morbidity and mortality, socioeconomic impact, geographic distribution and because it is a systemic disease with several therapeutic limitations (Campi-Azevedo et al., 2015; World Health Organization, 2015a). Also, this neglected disease has become a serious global health problem due to migratory flows of patients with Chagas disease from endemic countries to USA, Spain and other European countries forced medical staff to look for solutions to an emerging globalized problem (Cencig et al., 2012; Rassi et al., 2010). Even when there are currently about 25 million people at risk and > 8 million people infected, the Chagas disease has been and still remains a silent and silenced disease (Cencig et al., 2012; Rassi et al., 2010). Deprived of a successful treatment, the infection progresses to the chronic phase and it becomes lifelong threatening. Several years or even decades after the initial infection, about 30–40% of all infected people develop a chronic inflammatory disease that primarily affects the heart tissue (Coura and Borges-Pereira, 2012; Lo Presti et al., 2015; Rassi et al., 2010).

Currently, the efficacy and safety of Chagas disease chemotherapy is

* Corresponding author.
E-mail addresses: mgarcia@fcq.unc.edu.ar (M.C. García), mmartinelli@fcq.unc.edu.ar (M. Martinelli), nponce@fcq.unc.edu.ar (N.E. Ponce), lsanmarco@fcq.unc.edu.ar (L.M. Sanmarco), paoki@fcq.unc.edu.ar (M.P. Aoki), rubmanzo@fcq.unc.edu.ar (R.H. Manzo), alvaro@fcq.unc.edu.ar (A.F. Jimenez-Kairuz).

https://doi.org/10.1016/j.ejps.2018.04.034
Received 9 January 2018; Received in revised form 26 March 2018; Accepted 23 April 2018
Available online 27 April 2018
0928-0987/

still unsatisfactory and an effective prophylactic vaccine has yet to be developed (García et al., 2016). Benznidazole (BZ; Radanil®, LaRoche; Abarax®, Elea, Arg.) is one of two available drugs prescribed to treat the circulating form of the parasite (acute phase) of the infection (Bellera et al., 2015), with a parasitological cure rate of 60–80%, but its efficacy to treat the chronic stage of the disease is still controversial (Urbina, 2010).

Nevertheless, the chemotherapy with BZ presents some drawbacks and poor compliance, especially in adult patients, due to high dose and long-term treatment, frequent undesirable side effects and biochemical damage to mammalian tissues (Davies et al., 2014). In addition, BZ exhibits low aqueous solubility ($< 0.4\ mg.mL^{-1}$), which may produce low and/or variable bioavailability after oral administration.

Pharmaceutical technology has been working in order to solve some of the aspects of these problems by mean of the development of novel strategies employing new drug controlled release systems and/or formulations containing existing drugs (Bermudez et al., 2016; Chatelain and Ioset, 2011). Different kinds of drug delivery systems have been reported, including cyclodextrin complexes (de Melo et al., 2016; Leonardi et al., 2013; Soares-Sobrinho et al., 2012), oil/water emulsions (Streck et al., 2014), nano/microparticles and microcrystals (dos Santos-Silva et al., 2017; Leonardi et al., 2009; Maximiano et al., 2011), liposomal formulations (Morilla et al., 2002; Morilla et al., 2004), and solid dispersions (Fonseca-Berzal et al., 2015; Palmeiro-Roldán et al., 2014).

In particular, special interest has been focused on the development of oral multiparticulate drug delivery systems (MDDS) which involve matrix or coated drug particles based on one or more carrier polymers in order to control the release of the drug (Adeleke et al., 2014; AlHusban et al., 2011; Auriemma et al., 2013; Severino et al., 2012). Besides, MDDS offering several advantages over single-unit dosage forms, because of their multiplicity and small sizes including reduced risk of systemic toxicity, low risk of dose dumping, more uniform and reliable gastrointestinal transit, as each particle can be considered a true drug delivery system (AlHusban et al., 2011; Auriemma et al., 2013; Dey et al., 2008; Pan et al., 2010; Severino et al., 2012).

Interpolyelectrolyte complexes (IPEC) are macromolecular complexes obtained by the interaction of chemically complementary polymers, proton donors and acceptors, in which non-covalent interactions between oppositely charged polyions arise (Moustafine, 2014). In aqueous media, spontaneous and fast interactions occur at the first step of their formation, in which strong but reversible interactions take place, such as Coulomb forces; the second step involves the formation of new bonds to define the new conformation of the polymers chains and crosslinking occurs by mean of ionic bonds (de Robertis et al., 2015; Hennink and van Nostrum, 2012). However, other interactions such as hydrogen bonds or hydrophobic interactions may play an additional role. From an energetic point of view, IPEC formation may even be an endothermic process, because of the elastic energy contributions of the polyelectrolyte (PE) chains, which difficult the necessary conformational adaptations of the polymer chains during their transition to the much more compact (cross-linked) IPEC structure. In general, IPEC formation between polyions with strong ionic groups and similar molecular weights mixed in stoichiometric proportions results in insoluble complexes (Thünemann et al., 2004).

The use of IPEC for the development of MDDS has received remarkable attention in the recent years (*Bani*-Jaber et al., 2011; Mustafin et al., 2011; Obeidat et al., 2008; Prado et al., 2008). The IPEC have the capability to succeed more sustained drug release than single polymers (Bani-Jaberm et al., 2011; Jeganathan and Prakya, 2015) and have been used in an extensive variety of pharmaceutical applications, such as to improve the chemical and enzymatic stability of labile drugs, unpleasant tastes masking active compounds, enhance bioavailability by site/time specific drug release, and reduce the local irritation risk and patient-to-patient variability as a result of their more predictable gastric emptying and reproducible gastric residence time, and flexibility of blending units with different release patterns (AlHusban et al., 2011; Auriemma et al., 2013; Dey et al., 2008; Pan et al., 2010; Severino et al., 2012).

Eudragit® is part of the polymethacrylate family, and is extensively used in the pharmaceutical field to obtain IPEC due to its demonstrated low toxicity, high biocompatibility, easy availability and low cost (Mustafin, 2011; Patra et al., 2017). Several IPEC, containing different types and proportions of Eudragit® (L100–55, L100, S100, E100, EPO, among others), were prepared and studied for their potential use as drug delivery systems in different oral pharmaceutical dosage forms (Moustafine, 2014). In addition, drug-loaded IPEC nanodispersions based on the polymethacrylates Eudragit® EPO and L100 were described, showing improved drug delivery behavior in comparison to homologues binary complexes, and showed a remarkable robustness towards changes of pH in release media (from pH 1.2 to 6.8) (Palena et al., 2015; Palena et al., 2012).

Bearing in mind the advantageous properties that the IPEC exhibit, we hypothesize that this kind of system would be promising carriers of BZ, capable of overcoming the unfavorable properties of BZ, and therefore useful in the preparation of oral solid formulations with simple and low-cost procedures, would enable an interesting approach for developing new effective and safe BZ dosage forms in order to improve the current treatment of Chagas disease.

In this context, the goal of this work was to obtain novel MDDS composed by IPEC based on different polymethacrylate (Fig. 1) carriers loaded with BZ and to investigate their *in vitro* drug delivery performance for oral administration. Furthermore, the physicochemical characterizations were studied to evaluate the polymer-polymer and polymer-drug interactions. Preclinical studies in a murine model of acute Chagas disease were performed to evaluate the efficacy and safety of the MDDS in comparison to reference treatment.

2. Materials and methods

2.1. Materials: drug, polymers and reagents

The BZ was extracted and purified from commercially available tablets (Radanil®, Roche, Argentine), as reported in a previous work (García et al., 2016). Briefly, 100 tablets were crushed and the powder obtained was transferred into a glass container and dispersed with 2 mL of ethanol (Anedra®) per tablet under soft controlled heating (40–45 °C) and constant stirring for 30 min. After filtration, the remaining solid was discarded, and the BZ was recrystallized by the addition of 200 mL of cold distilled water under an ice bath condition. The solid was dried in oven at 45 °C until a constant weight was achieved and it stored at room temperature in well-closed light resistant glass containers. The crystalline solid was subjected to identification and purity analysis by Fourier transform infrared spectroscopy (FT-IR), differential scanning calorimetry (DSC) and high-performance liquid chromatography with UV–visible detection to ensure its quality as an active pharmaceutical ingredient.

Five polymethacrylates were supplied by Etilpharma (Bs. As., Arg.): Eudragit® EPO (EE), Eudragit® L100 (EL), Eudragit® L10055 (ELD), Eudragit® S100 (ES), and Eudragit® FS 30 D (EFS). The proportions of ionizable groups of these PE were determined by potentiometric titration and the equivalents of amino or carboxylic groups, expressed as $mmol.g^{-1}$ of PE were 3.15, 4.85, 4.28, 5.30, and 3.70 for EE, EL, ES, ELD and EFS, respectively. All determinations were performed by duplicate.

The following reagents: Na_3PO_4 KH_2PO_4 and K_2HPO_4 (PA grade, Anedra®), NaCl (PA grade, Parafarm®), absolute CH_3CH_2OH, 1 N NaOH and HCl solutions (Anedra®) and isofluoran (Forane®, Abbott, fractioned in Argentine) were used as purchased without further purification.

Physiological solution (sodium chloride 0.9% *w/v*), simulated gastric fluid without pepsin (SGF, to represent gastric pH in the fasted

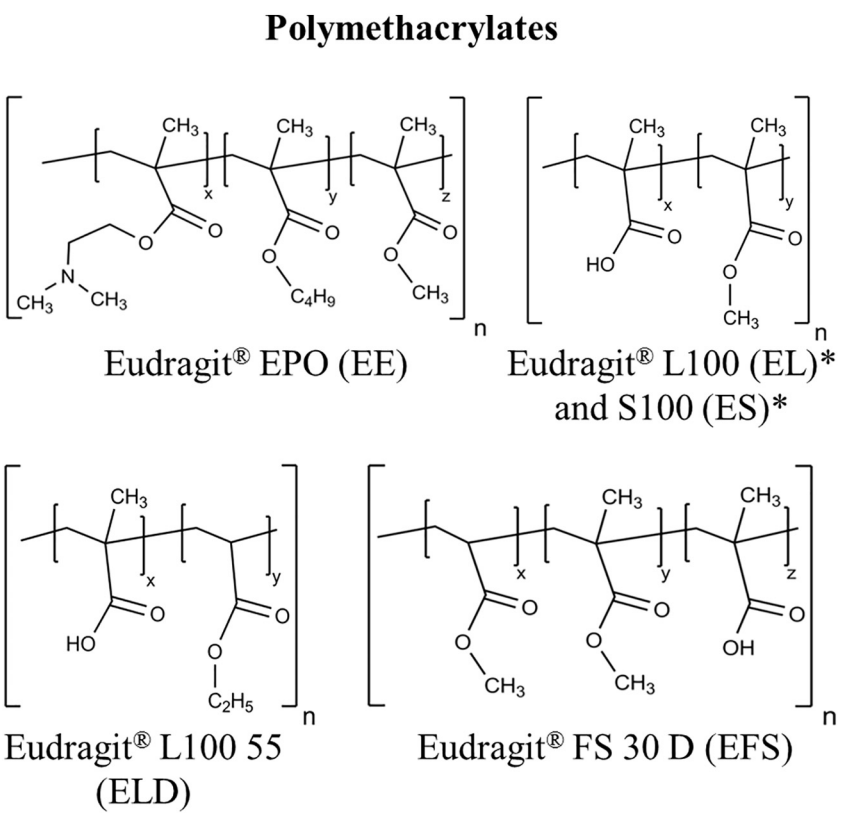

Fig. 1. Chemical structures of polyelectrolytes selected. *The ratio of the free carboxyl groups to the ester groups is approximately 1:1 in EL and 1:2 in ES.

state), and phosphate buffer pH 6.8 (to represent intestinal pH), were prepared according to the United States Pharmacopoeia specifications, using analytical grade reagents.

All experiments were carried out with distilled and purified water. For *in vivo* studies, sterilized water was employed.

2.2. Animals

Six to eight week-old male BALB/c mice, weighing 24 ± 3 g, were purchased from Universidad Nacional de La Plata (Argentine) and housed in the Animal Facility of the CIBICI-CONICET (OLAW Assurance number A5802–01). The animals had *ad libitum* access to water and feed. The experiments and procedures were carried out according to the guidelines of the Committee for Animal Care and Use of the Faculty of Chemical Sciences, National University of Cordoba, Argentine (Ethical Committee Approval Number HCD 753/14) in strict accordance with the recommendations of the Guide for the Care and Use of Experimental Animals published by the Canadian Council on Animal Care.

2.3. Preparation of BZ-loaded IPEC

Different IPEC composed of polymethacrylates were prepared following the steps represented in the scheme of Fig. S1 (Supplementary information). The EE was placed to interact with each of the acid polymethacrylates (EL, ELD, ES, EFS). The addition of the second PE was in stoichiometric proportions in order to neutralize all ionizable groups of the cationic PE. For that, the ionizable groups were determined by potentiometric titration, as previously described (Section 2.1). The BZ was incorporated in a ratio of 1:1 *w*/w respect to the total amount of IPEC. The stoichiometric proportions of anionic PE and the drug at each IPEC obtained are included in Table S1 (Supplementary material).

To obtain the solid state of these systems, the casting solvent method was employed. For that, the solids of the two PE and BZ were put in contact in a mortar and the interaction medium was added in small aliquots. Water and hydroalcoholic mixture (1:1 H_2O: CH_3CH_2OH) were used as interaction media. The selection of such solvents is based in previous studies, where pure ethyl alcohol and hydroalcoholic mixtures at different proportions of water and ethyl alcohol were assayed, and it was observed that high proportion of ethyl alcohol in the solvent mixture acts as plasticizer of the polymethacrylates yielding IPEC products with aspect of "rubbery materials", which were very difficult to process.

With the addition of the interaction medium, a semi-solid paste was formed, which was subjected to a mixing process during 10 min and left overnight at room temperature. The volume of media employed was (2.0 ± 0.4) and (1.7 ± 0.5) $mL.g^{-1}$ of solid, for water and hydroalcoholic medium, respectively. After 24 h, the material was dried at room temperature until a constant weight was achieved. It was considered constant when three successive determinations presented a mass variation < 5%. Once dry, the solid materials were milled and passed through in analytical sieves of 210 and 400 μm size pores (Fig. S1).

Finally, all the series of systems based on BZ-loaded IPEC systems were obtained in water (subscript *w*) and in hydroalcoholic medium (subscript *h*), namely EE-EL-BZ_w, EE-EL-BZ_h, EE-ELD-BZ_w, EE-ELD-BZ_h, EE-ES-BZ_w, EE-ES-BZ_h, EE-EFS-BZ_w and EE-EFS-BZ_h.

Physical mixtures (PM) with composition equivalents to the IPEC were prepared by a simple mixing of the powders in a mortar of the two PEs and BZ for each system.

2.4. Preparation of MDDS from BZ-loaded IPEC

The powders of BZ-loaded IPEC systems were subjected to a wet granulation process in order to obtain the MDDS. For this, each solid complex was placed in the mortar and was moistened with (42 ± 3)% *v/w* of water respect to the total amount of solid. After that, the multiparticles were obtained by extrusion of wet solids through an

850–1000 μm analytical sieve. The multiparticles were dried to a constant weight in an oven at 40 °C.

The MDDS were classified according to their particle size based on the analytical sieves used (mesh sieves: 1000–850 μm, 850–600 μm and ≤ 600 μm). The total amount of each fraction collated was summed and compared to the initial amount of solid used to obtain the IPEC, and the yield was determined. Also, the yield of each fraction collected was analyzed with respect to the total amount of each MDDS.

The MDDS of different particle sizes were packed into light-resistant glass containers for further characterization.

For physicochemical characterization and biopharmaceutical properties were determined mainly from MDDS 1000–850 μm fraction except to the comparison of release profiles of MDDS with different particle sizes.

2.5. Physicochemical characterization of BZ-loaded MDDS

Solid products IPEC, EE, EL, ES, EFS, BZ and their respective PM were characterized, at both molecular and particulated level, through confocal reflection microscopy, powder X-ray diffraction (p-XRD), FT-IR and thermal analysis.

2.5.1. Confocal reflection microscopy

Both MDDS based on IPEC obtained in water and hydroalcoholic media were analyzed using a confocal reflection microscope (LEXT OLS4000 3D Confocal Laser Microscope, Olympus®, Latin America). Specific software (Lext OLS 4000 version 3.1.1v, Olympus Corp) was used to take and process the images. Appropriate amount of samples (< 0.5 mg) with smallest particle sizes were prepared by carefully placing the solid material on a slide. Images were obtained with an increase of 408×.

2.5.2. Powder-X ray diffraction (p-XRD)

The p-XRD patterns were acquired at room temperature on an X-ray diffractometer (PANalytical® X'Pert Pro, Holland) using Cu Ka radiation (λ = 1.5418 Å, tube operated at 40 kV, 100 mA). Data were collected over an angular range from 5 to 45° 2θ/θ in continuous scan mode, with a step size of 0.02° 2θ and a time counting of 5 s per step. The obtained diffractograms were analyzed by an X'Pert data viewer (PANanalytical, Holland).

2.5.3. Fourier transform infrared spectroscopy

FT-IR spectra were acquired using an infrared microscope (Nicolet iN10, Thermo Scientific®, USA). The samples were dried under vacuum for 2 h before the determination. Appropriate amount of samples were placed on the pans and scanned from 4000 to 400 cm^{-1} and the recording conditions were resolution, 8.0; sample scan, 40. The spectra were obtained, processed and analyzed using the program EZ OMNIC ESP 5.1.

2.5.4. Thermal analysis

Thermal behavior was evaluated by DSC and thermogravimetric analysis (TGA) in a TA®-instrument, Discovery series equipped with a data station (Trios® software, v4.1.1, TA Instruments). DSC was performed on samples (0.9–1.7 mg) heated in non-hermetic aluminum pans with a pine hole, using heating ramp of 10 °C/min from 15 to 200 °C, under N_2 flux (50 mL.min^{-1}). TGA was performed on samples (approximately 2 mg) placed in open aluminum pans and heated from room temperature to 300 °C under the conditions used in DSC analysis.

2.6. Flow properties of particles

The flow properties of the MDDS were determined. The angle of repose (α) was determined according to Eq. (1).

$$tg(\alpha) = \frac{h}{r} \quad (1)$$

where h and r were height and base radius of the cone formed by the particles, respectively (Pérez et al., 2006). The bulk and tapped densities (δ_{bulk} and δ_{tap}, respectively) were determined; from these results, the Carr's Index (CI %) and Hausner's ratio (H_R) were calculated according to Eqs. (2) and (3), respectively, which are parameters to determine the flow properties of solids.

$$CI\% = \frac{\delta_{tap} - \delta_{bulk}}{\delta_{tap}} \times 100 \quad (2)$$

$$H_R = \frac{\delta_{tap}}{\delta_{bulk}} \quad (3)$$

All of these determinations were made using the methods described in the European Pharmacopoeia (European Pharmacopoeia, 2017). These experiments were carried out six times; mean values ± SD are reported.

2.7. Uptake measurements

The sorption (up-take) kinetics of water or SGF of 50 mg of MDDS based on the IPEC obtained in water as interaction medium were determined using an Enslin's apparatus as described by Nogami et al. (1969) (Nogami et al., 1969) at a room-controlled temperature. All assays were performed in triplicate and the fluid uptake was expressed in mL.

2.8. In vitro bioadhesion assay

The bioadhesion assay was performed by the mucin particle method (García et al., 2017; Takeuchi et al., 2005). In this study, pig gastric mucin was used. The mucin was suspended in USP phosphate buffer solution pH 7.4 and in SGF at a concentration of 0.1 mg.mL^{-1} and 3 mL of this suspension was placed in contact with (40 ± 2) mg of each solid at room temperature. After incubation for 48 h, the zeta potentials of mucin suspension in the absence of solids, and mucin suspension in contact with all the solids evaluated were measured in a Zetasizer Nano Series (Malvern®) and change values of the mucin particles due to the presence of the MDDS, BZ or polymers was an indication of bioadhesion (García et al., 2017).

2.9. Drug delivery studies

The BZ released from hard gelatin capsules (size 0) containing MDDS in proportion equivalent to 100 mg of BZ was evaluated. Due to we work on laboratory scale, the capsules were manually filled, one by one, with appropriate amount of BZ-loaded MDDS (approximately 200 mg). The release rate of BZ from the MDDS was measured in a rotating-basket dissolution apparatus (Sotax®AT 7 Smart, Switzerland) at 100 rpm and 37.0 ± 0.5 °C using 900 mL of degassed dissolution medium. Three different release assays were performed using three different release media. Distilled water and 0.9% NaCl solution media were used as two simple models of physiological fluids for evaluate the incidence of electrolytes on BZ release performance. To simulate gastrointestinal tract conditions, the "A" method encoded at the United States Pharmacopoeia (U.S. Pharmacopoeial Convention, 2015) to evaluate modified release dosage forms, which involves the evaluation of the release of BZ in acid medium for 2 h (HCl 0.1 M, 750 mL), followed by a simulated intestinal solution without enzymes for 4 h (phosphate buffer to achieve a final pH 6.8, 1000 mL) was employed. This change of pH is produced *in situ* in the dissolution vessel by the addition of 250 mL of 0.2 M Na_3PO_4 solution. The basket apparatus was selected to avoid floating of the capsules in the dissolution vessel. Standard baskets of 40# mesh size were used. Before each sampling

time, 10 mL of medium was taken out of the vessel, filtered through a Teflon® membrane (10 µm pore size) and then returned to the vessel in order to saturate the filter. Finally, samples of 5 mL were taken at defined time intervals, filtered through a Teflon® membrane and replaced with equivalent amounts of preheated fresh medium. BZ released was spectrophotometrically determined at 324 nm (UV–Vis Evolution 300 spectrophotometer, Thermo Electron Corporation, USA).

Particles with different sizes were analyzed for the MDDS based on EE-EL-BZ_h. The release assays were performed according to "A" method encoded at the United States Pharmacopoeia (U.S. Pharmacopoeial Convention, 2015).

In addition, MDDS composed of a mix of two IPEC were evaluated. For these studies, the MDDS based on EE-EL-BZ_w was incorporated in a proportion to represent 25% of the total amount of BZ, whereas the others systems selected EE-EL-BZ_h, EE-ELD-BZ_h, EE-ELD-BZ_w and EE-ES-BZ_h contributed the remaining 75% of BZ.

The results are presented as the cumulative percentage of BZ released as a function of time. All of the experiments were conducted in triplicate; mean values ± SD are reported.

The mean release profiles obtained in water and physiological solution were fitted according to following equations (Eqs. (4) and (5)) (Costa and Lobo, 2001; Siepmann and Peppas, 2001).

Eq. (4) is generally known as the simplified Higuchi model, in which the drug release is a diffusion process based in the Fick's law:

$$\frac{M_t}{M_0} = k \times t^{0.5} \tag{4}$$

where "M_t" is the amount of drug permeated at time "t", "M_0" is the initial amount of drug in the donor compartment and "k" is a constant reflecting structural and geometric characteristic of the device.

From linear analysis of the release profiles, plotting percentage of BZ release with respect to the square root of time, k_H was calculated and the correlation coefficients were determined (R^2).

The semi-empirical diffusion model (Eq. (5)), proposed by Peppas (Peppas, 1985), related the exponential drug release to the elapsed time and can be used to characterize different release mechanisms:

Eq. (5) proposed by Peppas allows the exponential drug release to be related to the elapsed time; this can be used to characterize different release mechanisms:

$$\frac{M_t}{M_0} = k \times t^n \tag{5}$$

where "M_t", "t", "M_0" and "k" were described above, and n is the release exponent characterizing the diffusional mechanism. For a slab, when n is 0.5, the fraction of drug released is proportional to the square root of time and the drug release is pure diffusion controlled; when n is 1, drug release is swelling controlled (zero order release kinetics or case-II transport). Values of n between 0.5 and 1 indicate anomalous transport and a superposition of both phenomena. This equation is valid in the release interval between 5 and 60% of the cumulated drug released. Plots of ln M_t/M_0 *versus* ln t were drawn, n and k values were calculated from the slopes and intercepts of the lines, respectively.

The correlation coefficient values (R^2) was used to compare the fit of the profiles using these kinetic models.

In addition, the release profiles of BZ from the MDDS were statistically compared using the similarity factor (f_2, Eq. (6)). According to this methodology, two profiles were considered similar when the f_2 value calculated between them was equal to or > 50. In other words, f_2 values between 50 and 100 guarantee likeness of the two release profiles (Costa and Lobo, 2001; Food and Drug Administration, 1997).

$$f_2 = 50 \cdot \log\left\{\left(1 + \left(\frac{1}{n}\right)\sum_{t=1}^{n}(R_t - P_t)^2\right)^{-0,5} \cdot 100\right\} \tag{6}$$

where log is the logarithm to base 10, n is the number of sampling time points, Σ is the summation of all time points and R_t and P_t are the cumulative percentages of drugs released at each of the n time points of the reference and test product, respectively.

2.10. Preclinical evaluation in a murine model of Chagas disease

2.10.1. In vivo assays in the acute phase of T. cruzi infection

BALB/c mice were infected intraperitoneally with 10^3 bloodstream trypomastigotes of *T. cruzi* (Tulahuen strain). For all treatment schedules, the drug or MDDS were administered by oral gavage for 14 days, starting the first dose 24 h after infection. Just before the oral administration, the treatments were dispersed into 30 µL of sterilized water. The animals were divided into groups of $n = 6$ and received free BZ or BZ-loaded IPEC at doses of 100 $mg \cdot kg^{-1} \cdot day^{-1}$. Non-infected animals (NI) and infected and non-treated mice (INT) were used as control. At 15 days post-infection (dpi) the animals were euthanized and blood samples were obtained and processed as it detailed in the following two sections.

2.10.2. Parasitemia and survival rate analysis

The mice were anesthetized with isofluorane and peripheral blood was extracted by intracardiac puncture. After 10 min with red blood lysis buffer the parasites were counted by direct microscopic observation in a Neubauer's chamber. Mouse survival was followed every day.

2.10.3. Tissue injury biochemical markers

Samples of blood were centrifuged at 2500 rpm for 5 min and the plasma was analyzed to determine the enzyme activities of glutamate oxaloacetate transaminase (GOT) and glutamate pyruvate transaminase (GPT) as liver injury biomarkers and from the relationship of them ($GOT.GPT^{-1}$) the De Ritis index was calculated (Davies et al., 2014). On the other hand, creatinphosphokinase (total CK) and creatinphosphokinase myocardial band isoform MB (CK-MB) as a cardiac injury marker were tested (Kindermann et al., 2012). These trials were outsourced to Biocon Laboratory (Cordoba, Argentina).

2.10.4. Statistical analysis

The statistical significance of comparisons of mean values was assessed by a two-tailed Student's *t*-test and, two-way ANOVA followed by Tukey's post-test using GraphPad software. A p-value < 0.05 was considered significant.

3. Results

The solid of BZ was obtained with yield of 87 ± 2%. FT-IR spectra showed the characteristics absorption bands of BZ, DSC curves demonstrated narrow melting temperature range at 190.2–191.2 °C (Figs. 4 and 5, respectively) and the quantification of BZ assayed by HPLC with UV detection exhibited 99.2 ± 0.5%p/p of BZ in the solid obtained (representative chromatogram in Fig. S2). These results agree with an acceptable purity of BZ according to Pharmacopoeia specifications (World Health Organization, 2015b).

The MDDS based BZ-loaded IPEC were developed by a two-step manufacturing process. The first step involved the casting solvent method to obtain BZ loaded-IPEC materials in a solid state using water or hydroalcoholic mixture as an interaction media. Then, powders of IPECs were wetted with purified water to obtain the MDDS by granulation. The wet granulation process allowed particles with different sizes to be obtained and the fractions collected (Retsch GmbH, 2017) presented as percentages recovered are shown in Table 1. These were obtained with yields of (83 ± 8)% with respect to the initial amount of powder used of PEs and BZ.

As shown in Table 1, the highest percentage recovered of MDDS was found in the fractions 850–1000 µm and 600–850 µm. In addition, it was observed that the interaction media presented a remarkable influence over the amount recovered for each fraction, but it was not observed a repetitive pattern between the interaction media and the

Table 1
Percentages recovered for each fraction of sizes of MDDS.

Multiparticulte IPEC	Fraction collected (%)		
	1000–850 μm	850–600 μm	≤ 600 μm
EE-EL-BZ$_w$	45.0	38.9	16.1
EE-EL-BZ$_h$	25.9	44.2	29.8
EE-ES-BZ$_w$	45.5	45.3	9.2
EE-ES-BZ$_h$	32.7	47.2	20.1
EE-ELD-BZ$_w$	84.0	10.8	5.2
EE-ELD-BZ$_h$	64.6	30.5	5.0
EE-EFS-BZ$_w$	40.7	42.4	16.9
EE-EFS-BZ$_h$	47.7	47.8	4.5

percentage recovered.

The macroscopic observations of the MDDS based on BZ-loaded IPEC obtained allow white color to be appreciated for the all of them, independent of the interaction medium. The particles appeared with a smooth or slightly porous surface.

3.1. Physicochemical characterization of MDDS

The confocal reflection microscopy allowed the superficial microscopic morphological features of the MDDS to be observed for the smallest sizes obtained (≤ 600 μm fractions). Fig. 2 (A and B) shows the images obtained for MDDS based on EE-EL-BZ, both complexes obtained in water and hydroalcoholic medium, represented on the left and right of each image, respectively. The particles of MDDS showed irregular topography in their surfaces. The coloration of the MDDS was white and homogeneous in most of the surface extension, but in some regions an increased intensity of coloration was observed corresponding to depression areas in the topography of particle surfaces. In addition, images corresponding to pure BZ and PM of polyelectrolytes and BZ are shown in Fig. 3 C and D, respectively. As can be seen, BZ in solid state is presented as acicular crystals and this form can be easily observed in the PM (Fig. 2 D).

The images of MDDS obtained in water as interaction media showed a higher proportion of crystalline BZ, but acicular crystals of smaller size than in PM can be observed on the surface of the particles. In contrast, for the IPEC obtained in hydroalcoholic medium, the proportion of BZ as a crystal was lower, observed by the presence of a lower quantity of acicular crystals in the particle surfaces analyzed.

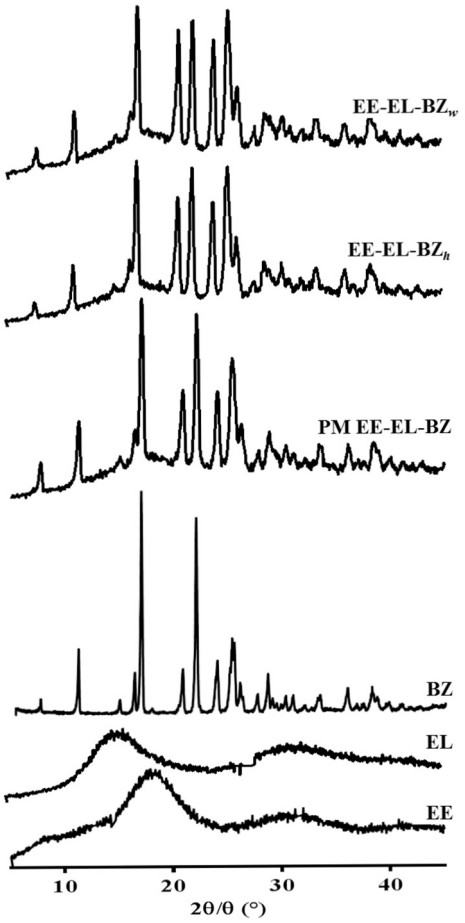

Fig. 3. Powder X-ray diffraction patterns of EE-EL-BZ interpolyelectrolyte complexes, their precursors and physical mixture (PM EE-EL-BZ).

The p-XRD patterns of all IPEC, pure PEs, BZ and their PM were performed (Fig. 3). The p-XRD profiles of BZ reveals the characteristic peaks of the crystalline form I of BZ at, 19.5°, 23.8°, 24.6° and 25.6° 2Θ/

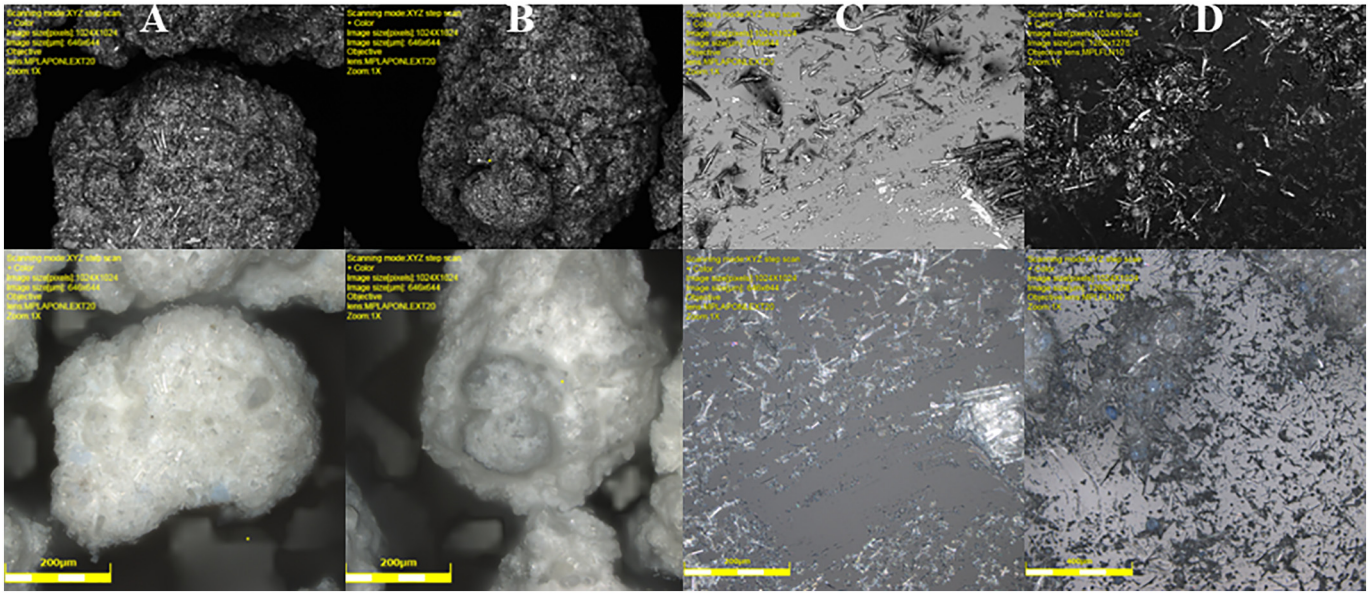

Fig. 2. Images obtained by confocal reflection microscopy (Scale bar: 200 μm) of the multiparticultate drug delivery systems (MDDS) based on EE-EL-BZ interpolyelectrolyte complex (IPEC) using A) water and B) hydroalcoholic as interaction media, C) crystalline BZ and D) physical mixture EE-EL-BZ.

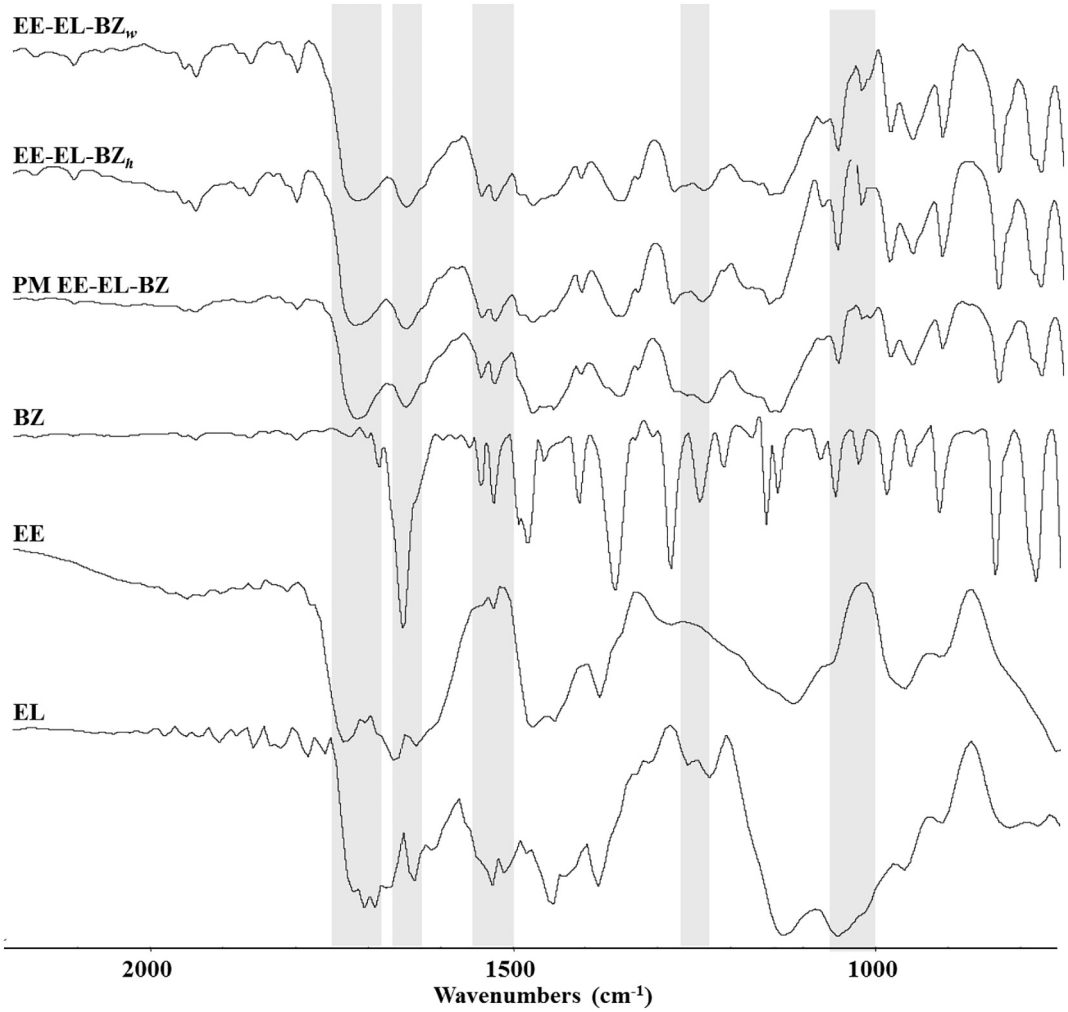

Fig. 4. FT-IR spectra of EE-EL-BZ interpolyelectrolyte complexes, their precursors and physical mixture (PM EE-EL-BZ).

Θ, in accordance with a previous report (Honorato et al., 2014). As can be seen, the p-XRD pattern of BZ was also observed in the IPEC based on EE-EL-BZ obtained in both interaction media and their PM, indicating that high proportion of BZ is presented as crystalline form even after the procedure applied to obtain the MDDS. No noticeable differences were observed between the p-XRD patters of the IPEC obtained in water or hydroalcoholic media. Similar results were obtained for the other IPEC (Supplementary material Fig. S4).

The samples were also analyzed by FT-IR and some differences in the band patterns were observed, as described below.

In the spectrum of BZ the region of 1555–1536 cm^{-1} can be assigned to in-plane N—H bend. A second, weaker band near to 1250 cm^{-1} also results from interaction between the N—H bending and C—N stretching. Moreover, the carbonyl stretching vibration (amide I band) is observed at 1658 cm^{-1} (Fig. 4).

The spectra of polymers (EE and EL) show the characteristic bands highlighting the band corresponding to carbonyl group (C=O) stretching vibration at higher frequencies (approx. 1700 cm^{-1}; Fig. 4). Also, the vibration characteristics of hydroxyl group (O—H) appear at approximately 3400 cm^{-1} as a wide band. Bands in the region 1000–1040 cm^{-1} can be observed, which can be associated with the C—O stretch coupled to the C—C stretch and O—H deformation (Wang and Somasundaran, 2006). Also, the asymmetric stretching vibration of CH_3 and CH_2 groups (approx. 2800 cm^{-1}) may be affected by intermolecular interactions between polymers chain and the drug loaded. In Fig. S3 can be noted that change of the hydration causes some spectral changes in the absorptions of C—H groups, which is evidenced by the two bands at 2822 and 2769 cm^{-1} clearly observed in the PM spectrum but not in the IPEC spectra (Dybal et al., 2009; Iwamoto and Murase, 2003; Lai and Wu, 2010).

The profile of bands corresponding to the spectra of both IPEC and PM shows the characteristic vibrations of the functional groups present in the polymers and BZ, according to Fig. 4. Similar results were obtained for the other IPEC (Supplementary material Fig. S6).

Fig. 5 A and B show the DSC and TGA curves, respectively, of both EE-EL-BZ IPECs, EE, EL, BZ and the PM. BZ crystalline form presents an intense endothermic peak (onset: 190.4 °C, maximum peak: 191.2 °C, ΔH = 124.3 J/g) without mass loss in TGA attributable to melting point. Neither moisture nor drug decomposition was detectable below 200 °C. In addition, in assay conditions the events corresponding to glass transition (*Tg*) of pure PE were not present. In the IPEC, the melting peak of BZ showed a small and wide endothermic transition, which is substantially lower than the expected one for the amount of BZ in the sample, showing ΔH values between 29 and 45 J/g. For all IPEC, the melting endothermic peak was followed by an exothermic event above 195 °C attributable to a decomposition process. The PM showed a similar endothermic peak corresponding to BZ melting, followed by component decomposition. However, PM showed ΔH values increased respect to IPEC material (between 59 and 72 J/g). In addition, the events corresponding to *Tg* did not show any differences with respect to those presented in pure precursor PE thermal curves. Analogous results were found for the other IPEC (Supplementary material Fig. S7).

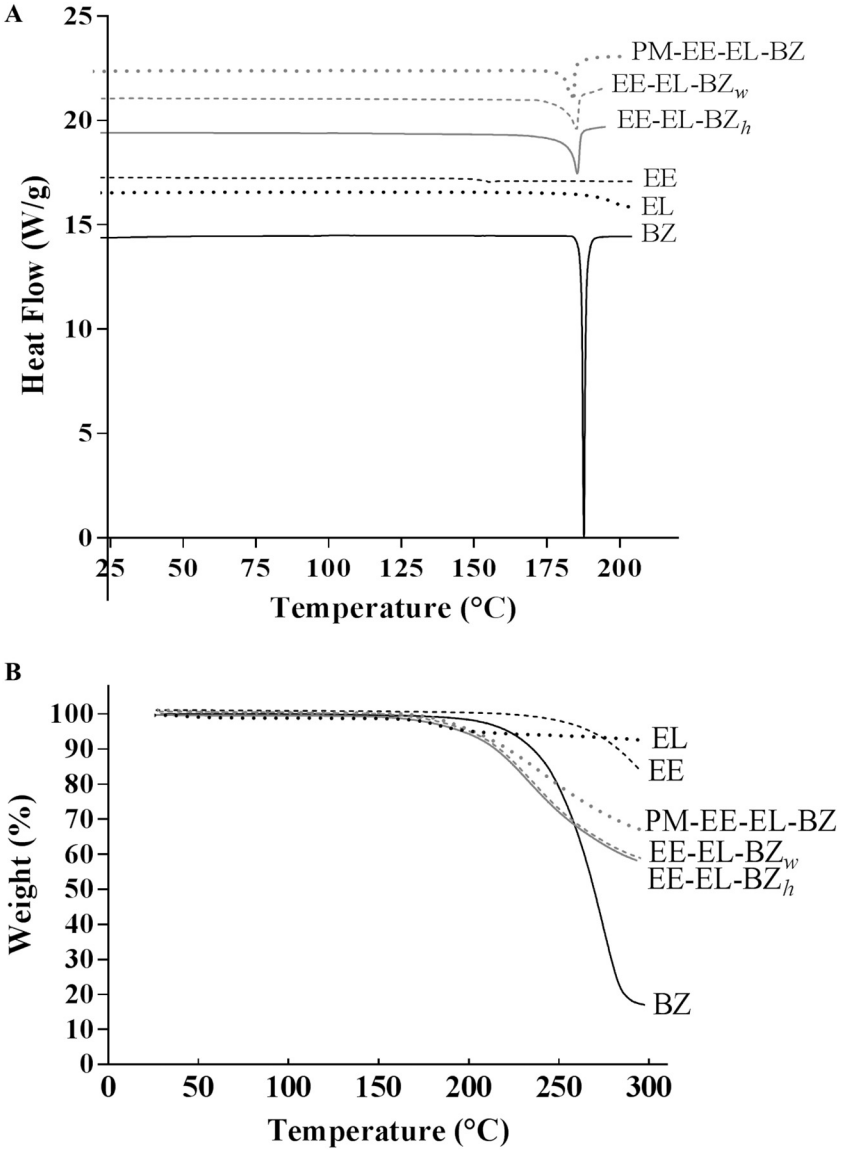

Fig. 5. A) DSC and B) TGA curves of EE-EL-BZ interpolyelectrolyte complexes, their precursors and physical mixture (PM EE-EL-BZ).

3.2. Flow properties of BZ-loaded MDDS

Table 2 shows the rheological properties of BZ and the MDDS corresponding to the highest fraction collected (850–1000 μm). As expected, the MDDS demonstrated significantly improved flow properties with respect to those of powder pure BZ and PE, which are adequate for the production of monolithic solid dosage forms, as capsules composed of multiparticles. In fact, according to European Pharmacopoeia scores, the Carr's Index and the Hausner's ratio of BZ changed in the IPEC from very poor to excellent and the angle of repose changed from poor to good or fair (European Pharmacopoeia, 2017) depending on the IPEC. No differences were observed between the flow parameters of the IPEC obtained in water or hydroalcoholic mixture as interaction media.

Table 2
Rheological properties of BZ and the MDDS based BZ-loaded IPEC with 850–1000 μm particle sizes.

Sample	Flow parameters				
	Bulk density ($g.mL^{-1}$)	Tap density ($g.mL^{-1}$)	Carr's Index	Hausner's ratio	Angle of repose (°)
BZ (powder)	0.11 ± 0.01	0.24 ± 0.02	54 ± 2	2.16 ± 0.03	52 ± 2
EE-EL-BZ_w	0.318 ± 0.004	0.339 ± 0.002	5 ± 2	1.05 ± 0.02	34 ± 2
EE-EL-BZ_h	0.41 ± 0.02	0.419 ± 0.009	2 ± 2	1.02 ± 0.02	34 ± 2
EE-ES-BZ_w	0.34 ± 0.01	0.41 ± 0.01	2 ± 2	1.02 ± 0.02	28 ± 2
EE-ES-BZ_h	0.34 ± 0.01	0.43 ± 0.01	3 ± 3	1.03 ± 0.03	30 ± 1
EE-ELD-BZ_w	0.37 ± 0.03	0.34 ± 0.02	7 ± 1	1.07 ± 0.01	31 ± 1
EE-ELD-BZ_h	0.40 ± 0.03	0.37 ± 0.02	6 ± 2	1.06 ± 0.02	30 ± 1
EE-EFS-BZ_w	0.34 ± 0.03	0.36 ± 0.03	6 ± 1	1.06 ± 0.01	32 ± 1
EE-EFS-BZ_h	0.38 ± 0.02	0.40 ± 0.03	5 ± 1	1.05 ± 0.01	35 ± 2

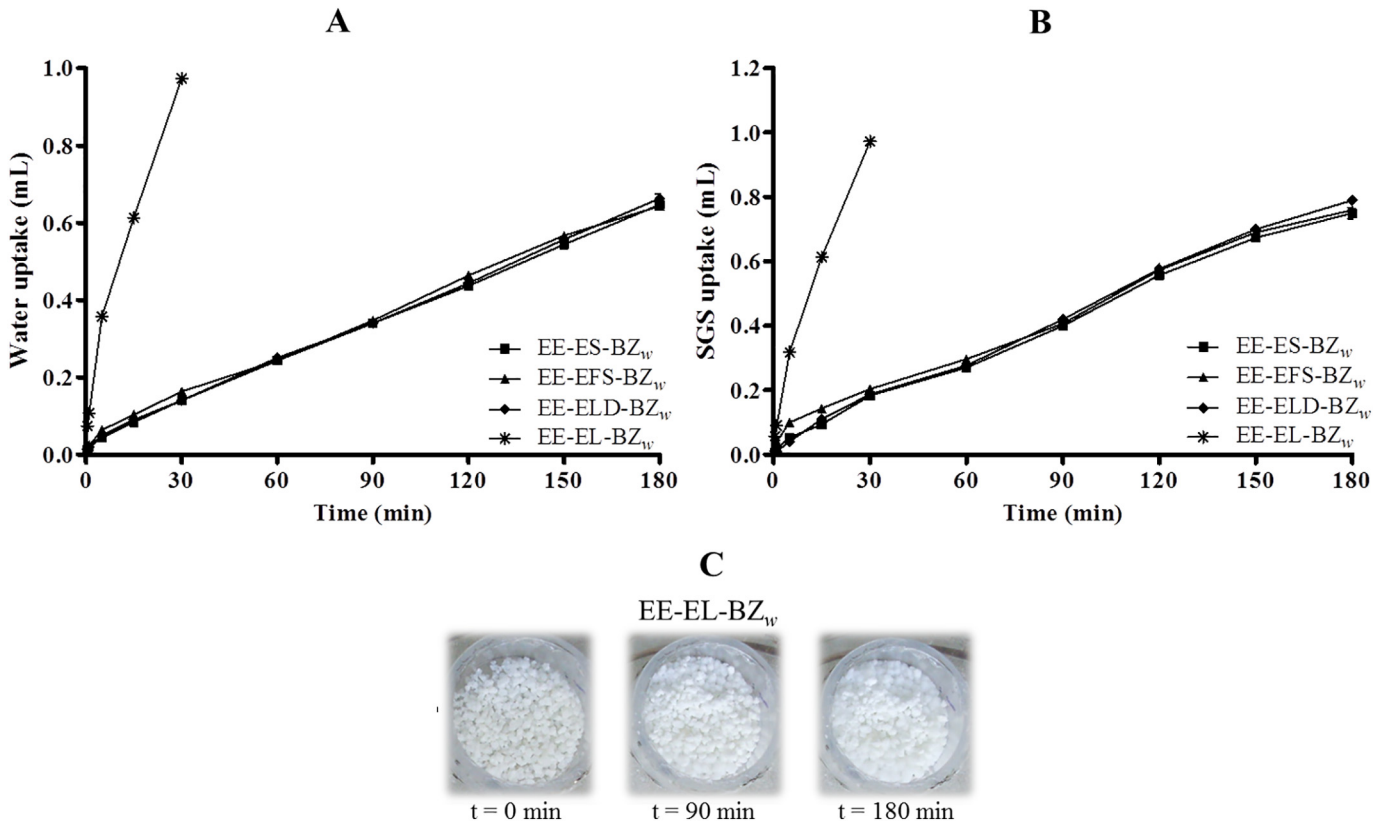

Fig. 6. Uptakes of A) water and B) SGF by 50 mg MDDS based on BZ-loaded interpolyelectrolyte complexes obtained in water as interaction medium. C) Images of the multiparticulate drug delivery systems based on EE-EL-BZ_w at different times of the assays of SGF uptake.

3.3. Fluid uptake by BZ-loaded MDDS

Water and SGF sorption were evaluated to assess the uptake of fluids by the MDDS based on the IPEC obtained in water as interaction medium using modified Enslin's apparatus, which allows the volume of liquid captured by capillarity at pre-established time intervals to be measured. Fig. 6 A and B show the sorption of fluids, water and SGF, respectively, by the MDDS obtained in water as an interaction medium. This assay was performed at room temperature at different times. The uptake profiles for EE-ELD-BZ_w, EE-ES-BZ_w and EE-ES-BZ_w were similar using water or SGF medium, showing a linear uptake as a function of time without an appreciable initial burst effect. For these complexes, the total amount taken up was approximately 0.7 mL after 180 min. Interestingly, the fluid sorption of EE-EL-BZ_w was very fast for the both fluids evaluated, reaching approximately 1 mL of both fluids captured in < 30 min. The sorption rates of fluids determined from the linear regression of the uptake profiles are presented in Table 2.

Table 3 revealed that the linear regressions for the sorption profiles were adequate due to the R^2 being higher than 0.97 in all the profiles evaluated. The results allow the observation that for EE-EL-BZ_w the sorption rate was approximately 10 times higher in comparison to the other BZ-loaded IPEC. Also, Fig. 6 C shows the macroscopic aspect of the MDDS based on EE-EL-BZ_w at 0, 90 and 180 min of the assays of water uptake, corresponding to the initial condition, middle time of the assay and final time evaluated, respectively. In these images, it can be observed that most of the particles contained in the hollow cylinder are wetted with SGF. For the EE-EL-BZ_w a limited swelling was observed. Similar appearances of the particles were observed when the sorption medium was water.

Table 3
Sorption rates of fluids determined from the linear regression of the uptake profiles for the MDDS based on IPEC obtained in water as interaction media. Slope expressed as (mean ± SD) mL.min^{-1}; R^2)

Sample	Fluids	
	Water	SGF
EE-EL-BZ_w	0.030 ± 0.001; 0.97	0.031 ± 0.001; 0.98
EE-ELD-BZ_w	0.00353 ± 0.00004; 0.99	0.00441 ± 0.00006; 0.99
EE-ES-BZ_w	0.00347 ± 0.00003; 0.99	0.00420 ± 0.00007; 0.99
EE-EFS-BZ_w	0.00345 ± 0.00004; 0.99	0.00407 ± 0.00008; 0,99

3.4. In vitro bioadhesion

The *in vitro* interaction of MDDS and their precursors with mucin was characterized by measuring the zeta potential of mucin suspension under equilibrium conditions. Mucin in aqueous dispersion, without solids, was used as a control in this assay. Fig. 7 shows the zeta potential under the different conditions evaluated. As seen, in phosphate buffer solution at pH 7.4 the mucin presented a negative charge due to the ionization of carboxyl groups, since environmental pH was higher than its pKa (pKa of mucin = 2.6). In the presence of MDDS and their precursors, the zeta potential of mucin dispersions changed to higher negative values (****$p < 0.001$ and **$p < 0.01$, Fig. 7A). Also, a significant difference was observed (****$p < 0.001$) between the MDDS obtained in water (EE-EL-BZ_w) and hydroalcoholic mixture (EE-EL-BZ_h) as interaction media; however, both present significant differences in comparison to pure mucin dispersion. An opposite behavior was observed in SGF, in which the zeta potential changed from negative to positive charge. In SGF mucin is under non-ionized form due to the pH of the medium was lower than its pKa, showing low zeta potential values (below to 6 mV). After interaction with both MDDS and EE higher values of zeta potential were observed, attributable to protonation of amine groups of EE (pKa = 8.4), but non-significant differences were evidenced between the MDDS based on EE-EL-BZ_w and EE-

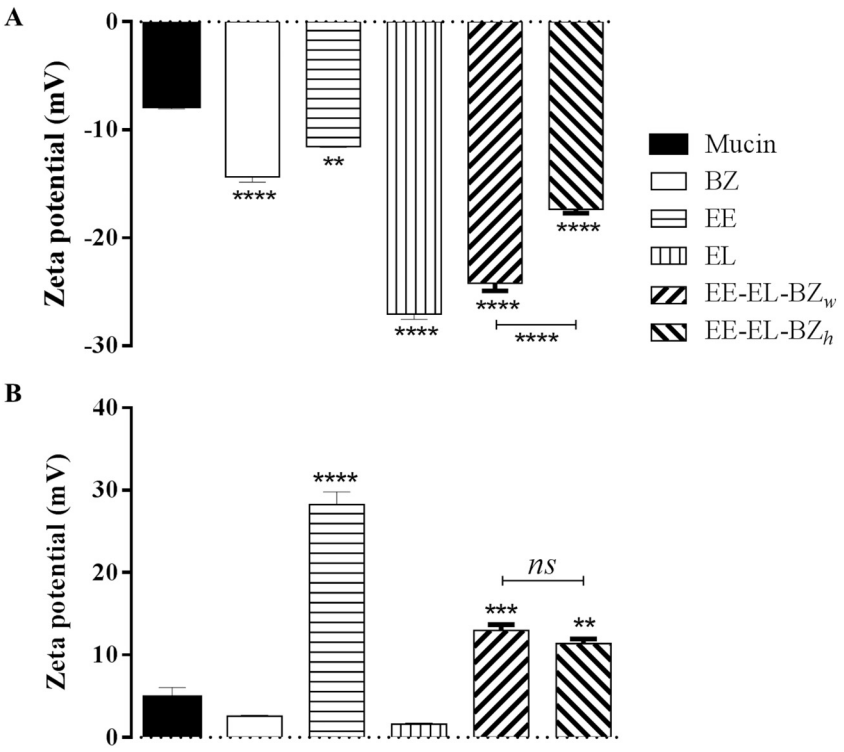

Fig. 7. Interactions of multiparticulate drug delivery systems (MDDS) based on EE-EL-BZ_w and EE-EL-BZ_h, inter-polyelectrolyte complexes and their precursors (EE, EL and BZ) with mucin by dynamic light scattering in A) buffer phosphate solution at pH 7.4 and B) simulated gastric fluid (SGF) without pepsin. Asterisks indicate a significant difference between the indicated groups respect to mucin (**** and ***$p < 0.001$ and **$p < 0.01$) and with the segment is presented a significant difference between the MDDS obtained in different media.

EL-BZ_h, Similar results were obtained for the other IPEC (Supplementary material Fig. S8).

3.5. In vitro drug release studies

The behavior of BZ release from MDDS was studied to evaluate its performance as an oral drug delivery dosage form. In the first instance, water and 0.9% NaCl solution were used as simple models of simulated physiological fluids in order to evaluate the main mechanisms involved in the release of BZ from the MDDS. On the other hand, specific pharmacopoeia methods were used to evaluate modified release dosage forms which simulate gastrointestinal tract conditions. Figs. 8A and B show BZ release profiles from MDDS towards water and physiological solutions, respectively. For all systems, slow and extended release BZ towards both receptor media was observed. The analysis of release profiles in water using the similarity test denoted that all the MDDS presented similar release profiles ($f_2 > 63$) reaching a cumulative BZ released up to 60%. Despite the statistical similarity between the BZ release profiles towards water, it can be observed that the BZ release rate followed the sequence EE-ELD-BZ_w > EE-ES-BZ_w ~ EE-EFS-BZ_w ~ EE-EL-BZ_w in the first 2 h of assay. When the receptor media was physiological solution it was no remarkable differences were observed between the release profiles of BZ from MDDS. However, the statistical analysis of these profiles allow the fact that only for EE-ES-BZ_w and EE-EFS-BZ_w were the release profiles similar ($f_2 > 74.98$) to be determined, while significant differences were observed with EL and ELD as counterPE. The BZ release rate followed the sequence: EE-ELD-BZ_w > EE-ES-BZ_w ~ EE-EFS-BZ_w > EE-EL-BZ_w, reaching a cumulative BZ released up to 65%, 50% and 30%, respectively.

Kinetic analyses of *in vitro* release data using Higuchi and Peppas equations were performed in order to evaluate the main mechanism of BZ transport through the polymeric matrix of MDDS. Results of kinetic analyses are summarized in Table 4. Drug release data plotted as Higuchi and Peppas model were found to be fairly linear for both of them and it was well supported by their regression coefficient values ($R^2 > 0.94$ and $R^2 > 0.96$, respectively).

Also, the n values confirmed that the kinetics of drug release in water from the MDDS, slightly near to 0.5, indicated a fickian transport with a preponderant release mechanism controlled by drug diffusion, in agreement with the good correlation coefficient obtained by application of the Higuchi model. Only BZ release towards water of MDDS based on EE-EFS-BZ_w showed an anomalous kinetic behavior ($n > 0.5$), in which kinetic control is resultant of both drug diffusion and polymer relaxation components.

Figs. 8 C and D show the release profiles of BZ from MDDS based on IPEC obtained in water and hydroalcoholic mixture, respectively, using method A-USP medium which simulate *in vitro* gastrointestinal transit (gastric environment, followed by intestinal environment). As it can be seen in Fig. 8 C, for the IPEC prepared with water, the BZ release properties had a remarkable influence of the system composition. The physicochemical properties of the counterPE produced differences in the release profiles of BZ in the first 2 h of these assays (gastric environment simulated). The BZ release rate followed the sequence: EE-EL-BZ_w > EE-ES-BZ_w > > EE-EFS-BZ_w > EE-ELD-BZ_w. It is important to highlight that the EE-ES-BZ_w showed an important "*burst effect*" and the BZ released reached the 65% at the first 5 min. After that, the release of BZ was controlled (intestinal environment simulated). For EE-EFS-BZ_w and EE-ELD-BZ_w the release of BZ was slow and controlled during the first 2 h. For the MDDS obtained in water, except EE-EL-BZ_w, the change in release media promoted the BZ release, which is in agreement with the increase in the apparent solubility of the polymethacrylates in buffer pH 6.8. Surprisingly, the EE-EL-BZ_w showed a very fast release of BZ, reaching the 90% in the first 5 min.

For the IPEC obtained in hydroalcoholic mixture (Fig. 8 D), during the first 2 h, the sequence of BZ release rate was as follow: EE-ES-BZ_h > EE-EL-BZ_h ~ EE-ELD-BZ_h > EE-EFS-BZ_h. Nevertheless, the release profiles showed fewer differences between them in comparison to the IPEC obtained in water. The EE-ES-BZ_h and EE-EL-BZ_h presented a significant reduction of "*burst effect*", reaching approximately 25% of the BZ-loaded MDDS in the first 5 min. For all systems, the release of BZ was sparingly promoted by the medium change, except for EE-EFS-BZ_h, where the influence in the change of medium was more remarkable.

Also, the analyses of the influence of the particle sizes in the release profiles of BZ were performed for EE-EL-BZ_h (Fig. 8 E). As expected, the

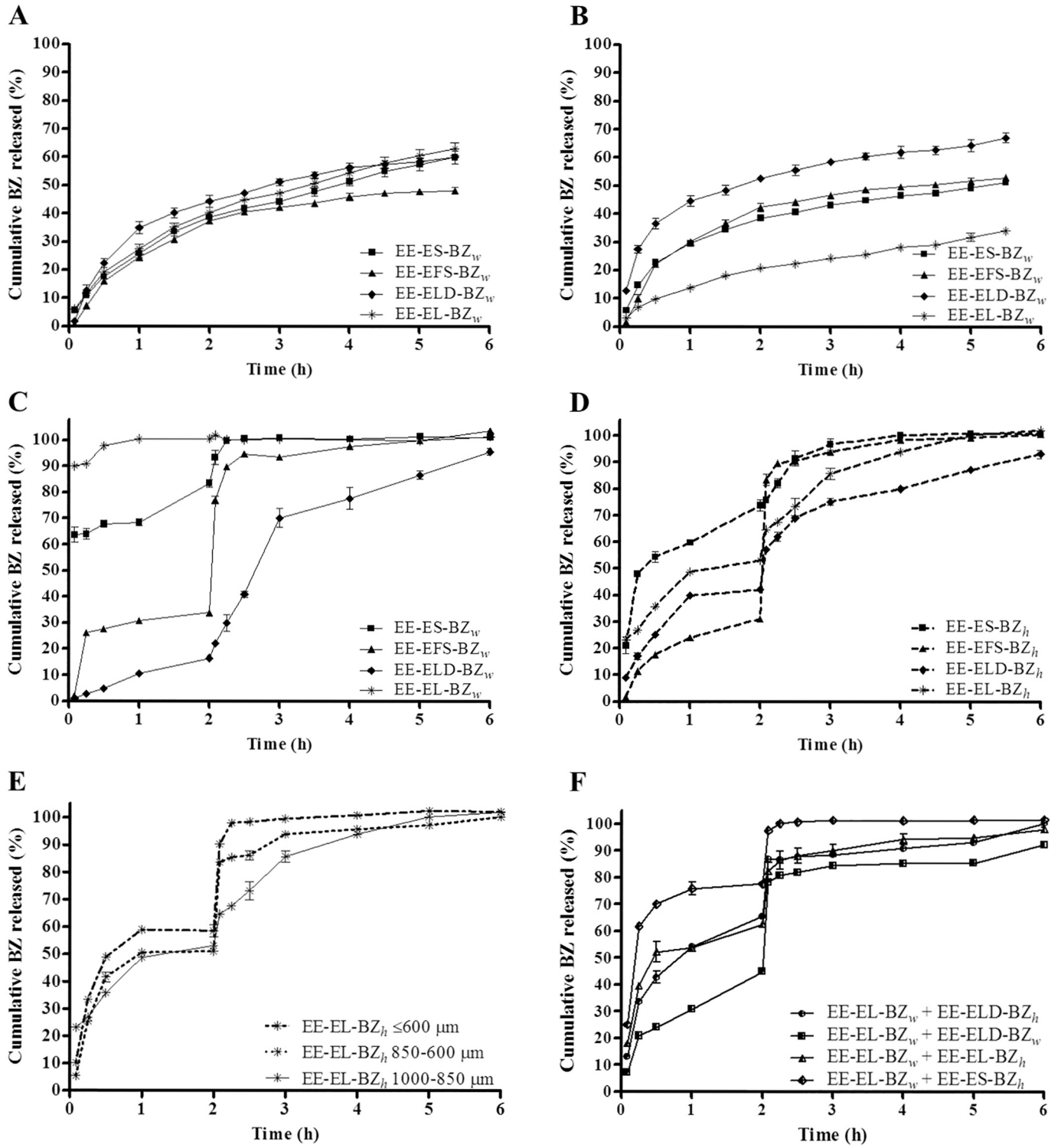

Fig. 8. Release profiles of BZ from multiparticulate drug delivery systems (MDDS) based on interpolyelectrolyte complexes obtained in water as an interaction media to A) water, B) physiological solution. Release profiles of BZ in method A-USP medium from MDDS based on IPEC obtained in C) water and D) hydroalcoholic mixture as an interaction media. Release profiles of BZ in method A-USP medium from MDDS of different particles sizes based on EE-EL-BZ_h interpolyelectrolyte complexes (E) and from combinations of two MDDS with individual different release profile (F).

amount of BZ released was sparingly higher at lower particle sizes.

Based on the results obtained for the BZ released in method A-USP medium, it was decided to evaluate the mixtures of two MDDS with different release profiles of BZ. As the BZ release behavior from EE-EL-BZ_w was particular, showing a very fast release, the combinations were made using this system plus other which exhibiting slow and controlled release of BZ as shown in Fig. 8 F. The proportion selected of each one was arbitrary. The EE-EL-BZ_w contributed with the 25% of the total amount of BZ and the other system with the remaining 75%. For all combinations evaluated, an initial "*burst effect*" reaching between 8 and 25% of BZ released in the first 5 min was observed. After that, the release was controlled for all the combined MDDS evaluated, and at 2 h

Table 4
Kinetic data obtained from drug release studies using Peppas equation.

Release media	Multiparticulate IPEC	Higuchi		Peppas	
		k	R^2	n	R^2
Water	**EE-EL-BZ$_w$**	26.53	0.99	0.50	0.99
	EE-ELD-BZ$_w$	24.35	0.96	0.48	0.96
	EE-ES-BZ$_w$	25.29	0.99	0.5	0.99
	EE-EFS-BZ$_w$	21.79	0.94	0.57	0.96
Physiological solution	**EE-EL-BZ$_w$**	14.15	0.99	0.51	0.99
	EE-ELD-BZ$_w$	23.04	0.98	0.29	0.99
	EE-ES-BZ$_w$	16.63	0.98	0.33	0.99
	EE-EFS-BZ$_w$	18.10	0.94	0.36	0.97

k expressed as %.h^{-1}. Experimental data corresponding to 5–60% of BZ released.
Eudragit EPO-Eudragit L100-benznidazole (EE-EL-BZ)$_w$; Eudragit EPO-Eudragit L10055-benznidazole (EE-ELD-BZ)$_w$; Eudragit EPO-Eudragit S100-benznidazole (EE-ES-BZ)$_w$; Eudragit EPO-Eudragit FS30D-benznidazole (EE-EFS-BZ)$_w$; the subscripts "w" or "h" refer to water or hydroalcoholic preparation method of IPEC, respectively.

when the medium was changed, the release of BZ was promoted reaching approximately 80% of BZ released at 6 h. In addition, it was observed that the BZ release profiles seem to be as summation of the individual release profile of each IPEC that composes the combined MDDS.

3.6. Preclinical studies

According to these results, the combination of EE-EL-BZ$_w$ + EE-EL-BZ$_h$ (BZ-loaded MDDS) was selected to be evaluated in a preliminary preclinical study, as a first attempt to assess the *in vivo* behavior of the developed systems. To this aim the treatment with BZ-loaded MDDS was evaluated in comparison to BZ at the reference dose (100 mg·kg^{-1}·day^{-1}) in a murine model of acute Chagas disease. It was observed that the reference treatment (Cencig et al., 2012) as well as BZ-loaded MDDS were able to override the parasitemia (Fig. 9 A). Moreover, both groups subjected to treatments and the healthy group (NI) presented lower ratio of plasma CK-MB/total CK enzyme activity in comparison to INT group ($p < 0.05$) (Fig. 9 B). Finally, the treatment with BZ at reference dose produced higher De Ritis Index than the other groups of animals ($p < 0.05$) (Fig. 9 C).

4. Discussion

The present work provides knowledge related to new pharmaceutical delivery systems based on polymeric carriers containing BZ to improve the current treatment of Chagas disease, specifically BZ-loaded MDDS based on IPEC composed by different Eudragit®. The physicochemical properties were studied as well as the rheological properties, fluid uptake, *in vitro* bioadhesion and BZ release performance. Also, in this paper we reported advantages related to the possibility of combine MDDS with different release profile for the loaded drug and preclinical studies in a murine model of acute Chagas disease were studied to assess the efficacy and security of the developed systems.

It has been previously reported the usefulness of MDDS for drug controlled release (Adeleke et al., 2014; AlHusban et al., 2011; Auriemma et al., 2013; Severino et al., 2012), where the polymer selected can provide different drug delivery behaviors. Indeed, MDDS offer several advantages over single-unit dosage forms, because of their multiplicity and small sizes including reduced risk of systemic toxicity, low risk of dose dumping, more uniform and reliable gastrointestinal transit (AlHusban et al., 2011; Auriemma et al., 2013; Dey et al., 2008; Pan et al., 2010; Severino et al., 2012).

It was observed that the MDDS has better flow than pure BZ, evaluated by the rheological properties of the MDDS (Table 2). The Carr's Index and the Hausner's ratio were excellent, and the angle of repose was good (European Pharmacopoeia, 2017), indicating that the MDDS obtained in both interaction media are adequate for the production of monolithic solid dosage forms as capsules (Vila Jato, 1997). It is important to highlight that the two step of manufacturing process used allows a very good yield for the MDDS (83 ± 8%) to be obtained, with respect to the initial amount of solid employed in their preparation (Table 1). It is important to highlight that simple methodologies were employed in order to obtain the BZ-loaded MDDS based on IPEC (Fig. 1).

The macroscopic observation of the MDDS showed that they have white color, in accordance with the coloration intrinsic characteristic that present the Eudragit®´s (Patra et al., 2017), and their surfaces were smooth or slightly porous (Fig. 2). However, the microscopic observation by confocal reflection microscopy made it possible to see that the

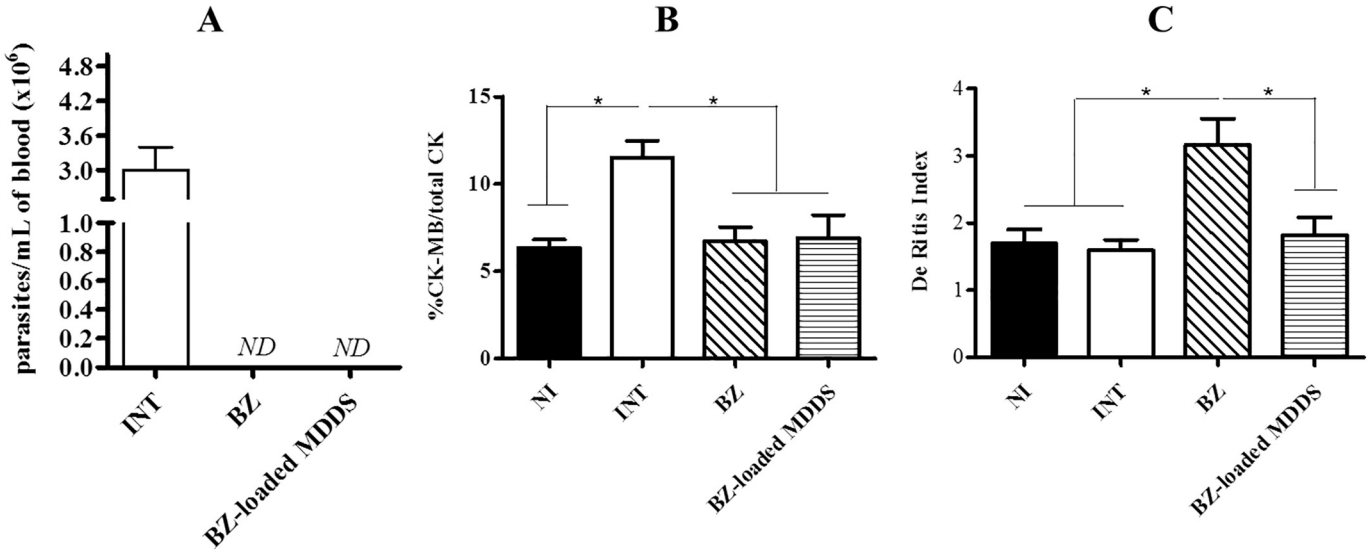

Fig. 9. Effects of BZ free drug at 100 mg·kg^{-1}·day^{-1} and BZ-loaded multiparticulate drug delivery systems (MDDS) based on interpolyelectrolyte complexes mix of EE-EL-BZ$_w$ + EE-EL-BZ$_h$ (contributing 25% and 75%, respectively, of the total dose of BZ 100 mg·kg^{-1}·day^{-1}) on A) Parasitemia, B) Relative percentage of CK-MB enzyme with respect to total CK in plasma and C) De Ritis index. The values were obtained at 15 dpi. Asterisks indicate a significant difference between the indicated groups and INT or BZ for %CKMB/total CK or De Ritis Index, respectively ($p < 0.05$).

MDDS possess irregular shapes and surfaces, and confirmed the white coloration of them, which is homogeneous in most of the surface extension. Nevertheless, some regions showed an increased intensity of coloration, corresponding to depression areas in the topography of particle surfaces (Fig. 2). The IPEC obtained in water as interaction media showed a higher proportion of crystalline BZ as acicular crystals on the surface of the particles, while the MDDS obtained in hydroalcoholic medium had a lower proportion of BZ as crystal. These differences can be observed due to the solubility of BZ in ethyl alcohol. In case of hydroalcoholic mixture as interaction media the proportion of soluble BZ is higher than when is used only water as interaction media. Then, as a greater proportion of BZ is dissolved, drug loading and interaction of the drug with the polymers is promoted and these allow good uniformity of BZ in the IPEC products. However, in both cases, a portion of free BZ was observed due to the drug crystals can be seen on the particle surfaces. These results are in accordance with the p-XRD obtained.

In this sense, it has been reported that traditional binary PE-drug complexes obtained by mixing a PE with an oppositely charged drug, in a convenient medium (water or ethanol) able to dissolve one or both components, result in solid amorphous materials where the drug is ionically bonded to the polymeric carrier (Olivera et al., 2017). Also, IPEC loaded with different drugs exhibited an absence of significant signals in the p-XRD, indicating that they have amorphous state (Mustafin, 2011; Mustafin et al., 2011; Palena et al., 2015; Palena et al., 2012). In contrast, BZ-loaded MDDS are crystalline material with sharp peaks observed by p-XRD (Fig. 3). This could be explained due to that BZ does not have ionizable groups in its chemical structure able to interact with the polymers; thus, BZ is molecularly dispersed in the MDDS into the polymeric matrix (Huang and Dai, 2014). Interestingly, evidence of acid-base reactions between both PE was observed (Fig. 4). The bands characteristics of BZ were more defined in the spectra corresponding to the PM than both IPEC obtained in water or hydroalcoholic media (Fig. 4). In the spectra of PM and IPEC, different relative intensities could be observed between the bands corresponding to the carbonyls groups of BZ (approx. 1660 cm^{-1}) and polymers (approx. 1700 cm^{-1}). Also, the hydrogen bonding would be expected to affect the C—O stretching and the changes in the infrared bands in the region 1000–1040 cm^{-1}, associated with the C—O stretch coupled to the C—C stretch and O—H deformation can be observed (Fig. 4) (Wang and Somasundaran, 2006).

These different patterns observed in the IPEC obtained in water or hydroalcoholic media could be due to the formation of hydrogen bonds between carbonyl groups of the polymers and amide groups of BZ. This interaction is less evident in PM. The spectra of IPEC show a shift in the band at 3400 to 3550 cm^{-1} (Fig. 4), consistent with the formation of intermolecular ionic bonds between ionized carboxylic acids of different counterpolyelectrolyte (counterPE, acid polymer) and EE protonated dimethylamines, in agreement with the literature that describes similar results for the other IPECs (Mustafin, 2011; Mustafin et al., 2011). However, the characteristic band at 1550–1560 cm^{-1} corresponding to the hydrogen bond would be overlapped with a band present in BZ, which presents a signal in the same region (1555–1536 cm^{-1} assigned to in-plane N—H bend) (Fig. 4). In addition, the asymmetric stretching vibration of CH_3 and CH_2 groups at about 2800 cm^{-1} may be affected by intermolecular interactions between polyelectrolyte chains and BZ. As it can be seen in Fig. S3, change of the hydration causes some spectral changes in the absorptions of C—H groups. Two bands at 2822 and 2769 cm^{-1} are clearly observed in the PM spectrum but the IPEC spectra revels that the hydrogen bonds could be partially destroyed and the vibrations corresponding to C—H bonds are less evident (Dybal et al., 2009; Iwamoto and Murase, 2003; Lai and Wu, 2010).

The DSC curve of pure BZ (Fig. 5), showed typical characteristics of a crystalline anhydrous solid with high purity, with a single and intense endothermic transition at about 191 °C, without mass loss in the TGA curve, related to the melting point of the drug (Lima et al., 2011). The thermal analysis showed that the IPEC exhibited a smaller wide endothermic peak of BZ, which corresponds to its melting point. That transition was ΔH values between 29 and 45 J/g, lower than expected respect to the amount of BZ in the sample. This thermal event was followed by an exothermic event attributable to a decomposition process (Fig. 5). In agreement with p-XRD and confocal microscopy results, in the PM was observed a similar endothermic peak corresponding to BZ melting, followed by component decomposition, but in this case with ΔH values higher than for the IPEC (between 59 and 72 J/g). These results indicate that even when a portion of BZ is free in the IPEC, there are interactions present between the BZ and polymers. In fact, according to FT-IR results BZ partially interacts with the polymer network as it was described above. Taking into consideration the ratio between the BZ experimental melting enthalpy from the PM and IPEC, respect to the pure drug, the proportion of drug that is molecularly dispersed or in crystalline form could be estimated. Thus, from PM and IPEC proportions of 35–50% and 65–50%, respectively, when compared with the melting enthalpy of pure BZ were observed.

On the other hand, in contrast to previous reports, the events corresponding to glass transition (*Tg*) of polymers were not observed (*Tg* values reported: EE $Tg = 48$ °C, EL and ES $Tg > 150$ °C, ELD $Tg = 110$ °C and EFS $Tg = 48$ °C 45), not only in the DSC curves of pure PE, but also in IPEC and PM (Patra et al., 2017).

The applicability of the new polymeric compounds as drug carriers could be determined by studying their swelling capacity in media imitating passage through the gastrointestinal tract (Mustafin et al., 2011). We studied the water and SGF sorption to assess the uptake of fluids by the MDDS using the Enslin's apparatus. Not noticeable differences were observed in the water or SGF uptakes by the MDDS. However, a remarkable increase in fluid uptakes was observed for the MDDS EE-EL-BZ_w, reaching very fast swelling properties. This represents sorption rates approximately 10 times higher than the others MDDS (Fig. 6 and Table 3). Interestingly, this behavior was in accordance with the release profile of BZ from the MDDS EE-EL-BZ_w to gastric environment simulated fluid (Fig. 8 C), in which a very fast release of BZ can be appreciated. In contrast, the release of BZ from EE-EL-BZ_h was more modulated (Fig. 8 D).

The release of BZ from MDDS towards water and physiological solution allow study of the kinetic mechanisms involved in its release. For all MDDS, the release of BZ was slow and extended (Fig. 8 A and B) and non-significant differences were observed in the release profile obtained in water as a receptor medium ($f_2 > 63$). Also, a fickian transport with a preponderant release mechanism controlled by drug diffusion was observed (Table 4), which is in agreement with the analysis using Higuchi and Peppas kinetic models. Also, BZ delivery towards physiological solution only EE-ES-BZ_w and EE-EFS-BZ_w exhibit similar release profile of BZ ($f_2 > 74.98$). In this medium, only the system based on EE-EFS-BZ_w showed an anomalous kinetic behavior, in which kinetic control is resultant of both drug diffusion and polymer relaxation components (Costa and Lobo, 2001; Siepmann and Peppas, 2001). Previous reports have described that the stability and swelling of the IPEC, as well as the release properties of the drug loaded are dependent on the ionic strength of the release media (Thünemann et al., 2004). It would have expected that due to the intermolecular ionic bonds between the PE that compose the IPEC (observed by FT-IR spectroscopy, Fig. 4), the presence of electrolytes in the physiological solution could promote substitution reactions (polyion exchange), decreasing the stability of the IPEC and increasing the release of the drug (Thünemann et al., 2004). However, there were no noticeable differences in the BZ released towards water or 0.9% NaCl.

Taking into consideration the similar ionogenic capacity and 1:1 stoichiometry of all the IPEC obtained, the higher BZ delivery from EE-ELD-BZ_w complex can be explained considering the existence of non-ionized dimethylamino groups in the IPEC, which indicates that in these structures the non-ionized groups of EE are localized mainly in

"defects" fields together with its ionized unbounded groups, which is largely dependent on the synthesis conditions. Thus, excess content of carboxyl copolymer chains (ELD) in the overall structure of originally "defective" IPEC obviously leads to a clustered segregation of hydrophobic regions of polyanion, with subsequent destruction of the IPEC (Moustafine and Bobyleva, 2006), which produce an increase in the BZ release rate. Intermediate behaviors between EE-EL-BZ$_w$ and EE-ELD-BZ$_w$ were observed for the IPEC composed by ES and EFS as counterPE. In general terms, non-significant changes in the BZ release rate towards saline solution respect to water was observed, which can be explained considering that BZ does not ionically interact with the PE and therefore ionic exchange with small electrolytes does not occur.

Complementary, the bioadhesion studies performed in both buffer phosphate solution at pH 7.4 and SGF (Fig. 7 A and B, respectively) showed significant changes in the zeta potential values of mucin dispersions at both pH evaluated, which are evidence that interactions occur between the solids evaluated and mucin, and thus revealing the bioadhesive properties of MDDS obtained in both interaction media (García et al., 2017). This property is important because provide many advantages, which include increased residence time at application sites, in this case in gastrointestinal tract, increased drug permeation, and improved drug availability (Bassi da Silva et al., 2017). All of these benefits allow improving the performance of the BZ-loaded MDDS.

Also, it was possible establish that the same components processed in different ways (using pure water or hydroalcoholic mixture as interaction media) allowed MDDS with different swelling and delivery performances to be obtained (Figs. 7 and 8 F). Previous reports described the importance of interaction medium composition on the IPEC formation and their properties (Thünemann et al., 2004). In this sense, more stable and stronger interaction between the PE that compose the IPEC could be obtained using hydroalcoholic mixture as interaction media, because PE are more soluble in this medium and a greater interpenetration (crosslinking points) between them can be achieved, which result in an IPEC with higher stability than that obtained using pure water as interaction media for complexation. As shown in Fig. 8D, the IPEC obtained in hydroalcoholic mixture showed higher robustness in the BZ release behavior towards simulated gastrointestinal conditions compared to those ones obtained in water as interaction media. Also, non-significant differences in the release profile of BZ were observed related to the composition of IPEC. Conversely, the IPEC obtained in water showed a wide range of BZ release profiles, which denote a higher sensitivity respect to the pH of the release media. In these cases, the MDDS showed bimodal BZ delivery. The IPECs based on EFS and ELD as counterPE, which are more hydrophobic Eudragit® showed higher modulation in the BZ release compared to ES and EL as counterPE. Also, the ES and EL possess higher number of ionogenic groups and methacrylic acid/methyl methacrylate which could explain the higher BZ release rate at acidic conditions (Mustafin, 2011). The results of fluid uptake (Fig. 6) were in agreement with the BZ release observed and the proportion of free BZ on the surface of particles (observed by confocal microscopy and p-XRD, Figs. 2 and 3, respectively) could describe the burst effect observed in the release profiles. In addition, the BZ may also be related to aqueous solubility of the counterPE, which are soluble at pH higher than 5.5, 7.0 and 7.2 for ELD, ES and EFS, respectively (Mustafin, 2011).

Considering the aforementioned, it would be highlighted that the BZ-loaded MDDS based on IPEC act as a reservoir of the drug and the combination of different bimodal drug release behavior can be used to design bioadhesive and multi-kinetic BZ delivery systems (Fig. 8F). In fact, the combination of the two different MDDS based on EE-EL-BZ$_w$ and EE-EL-BZ$_h$, EE-ELD-BZ$_h$, EE-ELD-BZ$_w$ or EE-ES-BZ$_h$, incorporated in a proportion to represent 25% and 75% of the total amount of BZ, respectively, allow obtaining combined MDDS which showed appropriate BZ release profiles that encouraged us to study its *in vivo* performance. As shown in Fig. 8F all combinations evaluated exhibited an initial "*burst effect*" produced by the very fast release of BZ from the MDDS based on EE-EL-BZ$_w$, followed by slow and controlled BZ release from the other systems that composed the combined MDDS, which revealed a pH-sensitive behavior and pulsatile by the microenvironment condition change, due to at 2 h, when the release media changed, from gastric environment simulated to intestinal environment simulated, the release of BZ was promoted in a single pulse reaching approximately 80% of BZ released. Bearing in mind this important approach and considering the differences in the BZ release profiles obtained, we decided to select the combination of the MDDS based on EE-EL-BZ obtained both in water and hidroalcoholic mixture as interaction media, because the same precursors allow obtaining different BZ release depending on the synthesis condition. The main advantage that would be exploited with this combined MDDS is in its *in vivo* performance, in which the initial BZ release would allow obtaining a sufficient dose to start its action against the parasites, followed by modulation in the release that would allow the maintenance of effective plasma concentrations of BZ. In this sense, it should be noted that several efforts have been made in the last two decades in order to develop drug formulations for infectious disease therapy. Some Eudragit such as EL and ELD have been employed for coating to release the drug in the upper part of the small intestine. This type of systems has been designed to provide a lag time followed by rapid release, and they are commonly known as delayed-release pulses (Saigal et al., 2009). Our combined MDDS take advantage of the properties that the polymethacrylates can offer for controlled drug release, but improve their performance due to in the first 2 h antiparasitic effect of BZ because of its initial release could be achieved.

In addition, several recent reports denote the great interest in the development of pharmaceutical drug delivery systems based on multiple unit dosage forms for different purposes. It is known that each particle or pellet based on IPEC or binary complexes can be considered a true drug delivery systems, which formulated as multiparticles would provide a more uniform and reliable gastrointestinal transit than single-unit dosage forms (Adeleke et al., 2014; AlHusban et al., 2011; Auriemma et al., 2013; Saigal et al., 2009; Severino et al., 2012). Thus, the *in vivo* performance of BZ from the combined MDDS would avoid dose dumping and reduce its side effect.

Preliminary *in vivo* studies using a model of experimental Chagas disease were used to evaluate the efficacy and safety of the BZ-loaded MDDS in comparison to free BZ at doses of 100 mg/kg/day. After infection, metacyclic trypomastigotes invade a wide range of host cells, where they transform into amastigotes. These forms undergo several cycles of binary division before transforming into infective trypomastigotes. Upon host cell burst, the trypomastigotes fall into the bloodstream. Thus, during the acute phase (which lasts for 2–4 months) the infection rate can be measured by determining the number of parasites into the peripheral blood (parasitemia). From the bloodstream the parasites are rapidly disseminated to multiple tissues, exhibiting a strong tropism for the myocardium and the liver (Aoki et al., 2012). While the rate of creatine kinase MB isozyme (CK-MB)/total CK, is a specific biochemical index of cardiac damage, De Ritis Index (the ratio between the plasma levels glutamate oxaloacetate transaminase (GOT) and glutamate pyruvate transaminase (GPT) provides useful information to measure the liver damage (García et al., 2016). Therefore, considering that the infection itself but also the BZ treatment could induce myocardium and hepatic damage we determined the %CK-MB/total CK and De Ritis Index as a measured of cardiac and liver injury, respectively.

The results obtained denoted that multi-kinetic BZ-loaded MDDS are efficient to override the parasitemia (Fig. 9A) and interestingly, they allow a reduction in De Ritis Index in comparison to BZ reference treatment, indicating a reduction on the liver damage (Fig. 9C) (Davies et al., 2014). Thus, although the efficacy of both evaluated treatments was similar, the MDDS could provide more safety for Chagas pharmacotherapy. This first attempts encourage us to propose more challenged studies to evaluate the potential use of the systems in the treatment of Chagas disease.

In conclusion, BZ-loaded MDDS based on novel IPECs composed of biocompatible Eudragit®, using simple manufacturing methods, yielded physical and stable products. The MDDS showed bioadhesive properties and also an extended pH-sensitive release of BZ, in which delivery properties change depending on the composition of the systems. Multikinetic release of BZ for capsules containing a combination of two MDDS with different release profile of BZ was observed and they showed promising properties to improve Chagas disease pharmacotherapy in the preliminary *in vivo* assay performed. The *in vivo* studies showed that BZ-loaded MDDS exhibited efficacy to reduce parasitemia, while decreasing the levels of liver injury markers in comparison to BZ conventional treatment. Thus, the BZ delivery systems showed promising properties and could be interesting pharmaceutical alternatives to improve the pharmacotherapy of Chagas disease.

Acknowledgements

Martinelli M, Aoki MP, Manzo RH and Jimenez-Kairuz AF are members of CONICET scientific career. García MC and Ponce NE thank to CONICET postdoctoral fellowships and Sanmarco LM thanks to CONICET doctoral fellowship.

Authors thank Mgter. Norma Maggia (Laboratorio de Análisis Térmico, UNITEFA, CONICET-UNC) for technical assistance and perform of DSC-TGA runs. Also, authors would like to thank Etilfarma S.A. (Evonik, Argentine) for the provision of Eudragit® and Coordinación Nacional de Control de Vectores and Ministerio de Salud de la Nación (filial Córdoba) for supplying the Radanil® tablets used to do this work.

Special thank at the professional editing and proofreading of this document made by Proof-Reading-Service.com, ensuring consistency of the spelling, grammar and punctuation.

Funding sources

This work was supported by Agencia Nacional de Promoción Científica y Tecnológica – Fondo para la investigación Científica y Tecnológica (Grant number FONCyT-program, PICT 2012-0173); Consejo Nacional de Investigaciones Científicas y Técnicas de la República Argentina (Grant number: CONICET, PIP 2013-2016, No: 11220120100461); Secretaría de Ciencia y Tecnología. Universidad Nacional de Córdoba (Grant number: SECyT-UNC, 2014-2016, No: 30720130100922CB).

Appendix A. Supplementary data

Scheme for obtaining the BZ-loaded MDDS and a table detailing the stoichiometric proportions of anionic PE and the drug at each IPEC obtained were included as Fig. S1 and Table S1, respectively.

A representative chromatogram of an aqueous solution of BZ extracted and purified from commercial available tablets is provided as Fig. S2, in which only one peak is observed, indicating the high purity of the solid obtained.

Figures of confocal microscopy, p-XRD, FT-IR and thermal analysis of IPEC, its physical mixtures and polymethacrylates Eudragit S100 (ES), L100–55 (ELD) and FS30D (EFS) are provided (Figs. S3–7). Zeta potential of mucin dispersions after interaction with those polyelectrolytes and their respective IPEC are also provided (Fig. S8).

References

Adeleke, O.A., Choonara, Y.E., Du Toit, L.C., Pillay, V., 2014. In vivo and ex vivo evaluation of a multi-particulate composite construct for sustained transbuccal delivery of carbamazepine. J. Pharm. Sci. 103, 1157–1169.

AlHusban, F., Perrie, Y., Mohammed, A.R., 2011. Formulation of multiparticulate systems as lyophilised orally disintegrating tablets. Eur. J. Pharm. Biopharm. 79, 627–634.

Aoki, M., Carrera-Silva, E., Cuervo, H., Fresno, M., Girones, N., Gea, S., 2012. Nonimmune cells contribute to crosstalk between immune cells and inflammatory mediators in the innate response to Trypanosoma cruzi infection. J. Parasitol. Res. 2012, 1–13.

Auriemma, G., Mencherini, T., Russo, P., Stigliani, M., Aquino, R.P., Del Gaudio, P., 2013. Prilling for the development of multi-particulate colon drug delivery systems: pectin vs. pectin–alginate beads. Carbohydr. Polym. 92, 367–373.

Bani-Jaber, A., Al-Aani, L., Alkhatib, H., Al-Khalidi, B., 2011. Prolonged intragastric drug delivery mediated by Eudragit® E-carrageenan polyelectrolyte matrix tablets. AAPS PharmSciTech 12, 354–361.

Bani-Jaberm, A.K., Alkawareek, M.Y., Al-Gousous, J.J., Abu Helwa, A.Y., 2011. Floating and sustained-release characteristics of effervescent tablets prepared with a mixed matrix of Eudragit L-100-55 and Eudragit E PO. Chem. Pharm. Bull. 59, 155–160.

Bassi da Silva, J., Ferreira, S.B.d.S., de Freitas, O., Bruschi, M.L., 2017. A critical review about methodologies for the analysis of mucoadhesive properties of drug delivery systems. Drug Dev. Ind. Pharm. 43, 1053–1070.

Bellera, C., Sbaraglini, M., Balcazar, D., Fraccaroli, L., Cristina Vanrell, M., Florencia Casassa, A., Labriola, C., Romano, P., Carrillo, C., Talevi, A., 2015. High-throughput drug repositioning for the discovery of new treatments for Chagas disease. Mini-Rev. Med. Chem. 15, 182–193.

Bermudez, J., Davies, C., Simonazzi, A., Real, J.P., Palma, S., 2016. Current drug therapy and pharmaceutical challenges for Chagas disease. Acta Trop. 156, 1–16.

Campi-Azevedo, A., Gomes, J., Teixeira-Carvalho, A., Silveira-Lemos, D., Vitelli-Avelar, D., Sathler-Avelar, R., Peruhype-Magalhaes, V., Bela, S., Silvestre, K., Batista, M., Schachnik, N., Correa-Oliveira, R., Eloi-Santos, S., Martins-Filho, O., 2015. Etiological treatment of Chagas disease patients with benznidazole lead to a sustained pro-inflammatory profile counterbalanced by modulatory events. Immunobiology 220, 564–574.

Cencig, S., Coltel, N., Truyens, C., Carlier, Y., 2012. Evaluation of benznidazole treatment combined with nifurtimox, posaconazole or AmBisome(R) in mice infected with Trypanosoma cruzi strains. Int. J. Antimicrob. Agents 40, 527–532.

Chatelain, E., Ioset, J., 2011. Drug discovery and development for neglected diseases: the DNDi model. Drug Des. Devel. Ther. 5, 175–181.

Costa, P., Lobo, J.M.S., 2001. Modeling and comparison of dissolution profiles. Eur. J. Pharm. Sci. 13, 123–133.

Coura, J., Borges-Pereira, J., 2012. Chagas disease. What is known and what should be improved: a systemic review. Rev. Soc. Bras. Med. Trop. 45 (3), 286–296.

Davies, C., Dey, N., Negrette, O., Parada, L., Basombrio, M., Garg, N., 2014. Hepatotoxicity in mice of a novel anti-parasite drug candidate hydroxymethylnitrofurazone: a comparison with Benznidazole. PLoS Negl. Trop. Dis. 8, 1–12.

Dey, N., Majumdar, S., Rao, M., 2008. Multiparticulate drug delivery systems for controlled release. Trop. J. Pharm. Res. 7, 1067–1075.

dos Santos-Silva, A.M., de Caland, L.B., de SL Oliveira, A.L.C., de Araújo-Júnior, R.F., Fernandes-Pedrosa, M.F., Cornélio, A.M., da Silva-Júnior, A.A., 2017. Designing structural features of novel benznidazole-loaded cationic nanoparticles for inducing slow drug release and improvement of biological efficacy. Mater. Sci. Eng. C 78, 978–987.

Dybal, J., Trchová, M., Schmidt, P., 2009. The role of water in structural changes of poly (N-isopropylacrylamide) and poly (N-isopropylmethacrylamide) studied by FTIR, Raman spectroscopy and quantum chemical calculations. Vib. Spectrosc. 51, 44–51.

European Pharmacopoeia, P.E., 2017. European Pharmacopoeia 8th Edition. European Directorate for the Quality of Medicines & HealthCare, Council of Europe 7 allée Kastner, CS 30026.

Fonseca-Berzal, C., Palmeiro-Roldán, R., Escario, J.A., Torrado, S., Arán, V.J., Torrado-Santiago, S., Gómez-Barrio, A., 2015. Novel solid dispersions of benznidazole: preparation, dissolution profile and biological evaluation as alternative antichagasic drug delivery system. Exp. Parasitol. 149, 84–91.

Food and Drug Administration, 1997. Guidance for Industry: Dissolution Testing of Immediate-release Solid Oral Dosage Forms. Food and Drug Administration, Center for Drug Evaluation and Research (CDER).

García, M.C., Ponce, N.E., Sanmarco, L.M., Manzo, R.H., Jimenez-Kairuz, A.F., Aoki, M.P., 2016. Clomipramine and Benznidazole act synergistically and ameliorate the outcome of experimental Chagas disease. Antimicrob. Agents Chemother. 60, 3700–3708.

García, M.C., Aldana, A.A., Tártara, L.I., Alovero, F., Strumia, M.C., Manzo, R.H., Martinelli, M., Jimenez-Kairuz, A.F., 2017. Bioadhesive and biocompatible films as wound dressing materials based on a novel dendronized chitosan loaded with ciprofloxacin. Carbohydr. Polym. 175, 75–86.

Hennink, W.E., van Nostrum, C.F., 2012. Novel crosslinking methods to design hydrogels. Adv. Drug Deliv. Rev. 64, 223–236.

Honorato, S.B., Mendonça, J.S., Boechat, N., Oliveira, A.C., Mendes Filho, J., Ellena, J., Ayala, A.P., 2014. Novel polymorphs of the anti-Trypanosoma cruzi drug benznidazole. Spectrochim. Acta A Mol. Biomol. Spectrosc. 118, 389–394.

Huang, Y., Dai, W.-G., 2014. Fundamental aspects of solid dispersion technology for poorly soluble drugs. Acta Pharm. Sin. B 4, 18–25.

Iwamoto, R., Murase, H., 2003. Infrared spectroscopic study of the interactions of nylon-6 with water. J. Polym. Sci. B Polym. Phys. 41, 1722–1729.

Jeganathan, B., Prakya, V., 2015. Interpolyelectrolyte complexes of Eudragit® EPO with hypromellose acetate succinate and Eudragit® EPO with hypromellose phthalate as potential carriers for oral controlled drug delivery. AAPS PharmSciTech 16, 878–888.

Kindermann, I., Barth, C., Mahfoud, F., Ukena, C., Lenski, M., Yilmaz, A., Klingel, K., Kandolf, R., Sechtem, U., Cooper, L., Bohm, M., 2012. Update on myocarditis. J. Am. Coll. Cardiol. 59, 779–792.

Lai, H., Wu, P., 2010. A infrared spectroscopic study on the mechanism of temperature-induced phase transition of concentrated aqueous solutions of poly (N-isopropylacrylamide) and N-isopropylpropionamide. Polymer 51, 1404–1412.

Leonardi, D., Salomón, C.J., Lamas, M.C., Olivieri, A.C., 2009. Development of novel formulations for Chagas' disease: optimization of benznidazole chitosan

microparticles based on artificial neural networks. Int. J. Pharm. 367, 140–147.
Leonardi, D., Bombardiere, M.E., Salomon, C.J., 2013. Effects of benznidazole: cyclodextrin complexes on the drug bioavailability upon oral administration to rats. Int. J. Biol. Macromol. 62, 543–548.
Lima, Á.A., Soares-Sobrinho, J.L., Silva, J.L., Corrêa-Júnior, R.A., Lyra, M.A., Santos, F.L., Oliveira, B.G., Hernandes, M.Z., Rolim, L.A., Rolim-Neto, P.J., 2011. The use of solid dispersion systems in hydrophilic carriers to increase benznidazole solubility. J. Pharm. Sci. 100, 2443–2451.
Lo Presti, M., Bazan, P., Strauss, M., Baez, A., Rivarola, H., Paglini-Oliva, P., 2015. Trypanothione reductase inhibitors: overview of the action of thioridazine in different stages of Chagas disease. Acta Trop. 145, 79–87.
Maximiano, F., de Paula, L., Figueiredo, V., de Andrade, I., Talvani, A., Sa-Barreto, L., Bahia, M., Cunha-Filho, M., 2011. Benznidazole microcrystal preparation by solvent change precipitation and in vivo evaluation in the treatment of Chagas disease. Eur. J. Pharm. Biopharm. 78, 377–384.
de Melo, P.N., Barbosa, E.G., Garnero, C., de Caland, L.B., Fernandes-Pedrosa, M.F., Longhi, M.R., da Silva-Júnior, A.A., 2016. Interaction pathways of specific co-solvents with hydroxypropyl-β-cyclodextrin inclusion complexes with benznidazole in liquid and solid phase. J. Mol. Liq. 223, 350–359.
Morilla, M.J., Benavidez, P., Lopez, M., Bakas, L., Romero, E., 2002. Development and in vitro characterisation of a benznidazole liposomal formulation. Int. J. Pharm. 249, 89–99.
Morilla, M.J., Montanari, J., Prieto, M., Lopez, M., Petray, P., Romero, E., 2004. Intravenous liposomal benznidazole as trypanocidal agent: increasing drug delivery to liver is not enough. Int. J. Pharm. 278, 311–318.
Moustafine, R., 2014. Role of macromolecular interactions of pharmaceutically acceptable polymers in functioning oral drug delivery systems. Russ. J. Gen. Chem. 84, 364–367.
Moustafine, R., Bobyleva, O., 2006. Design of new polymer carriers based of Eudragit® E PO/Eudragit® L100-55 interpolyelectrolyte complexes using swellability measurements. J. Control. Release 116, 35–36.
Mustafin, R., 2011. Interpolymer combinations of chemically complementary grades of Eudragit copolymers: a new direction in the design of peroral solid dosage forms of drug delivery systems with controlled release (review). Pharm. Chem. J. 45, 285–295.
Mustafin, R., Bukhovets, A., Sitenkov, A.Y., Garipova, V., Kemenova, V., Rombaut, P., Van den Mooter, G., 2011. Synthesis and characterization of a new carrier based on Eudragit® EPO/S100 interpolyelectrolyte complex for controlled colon-specific drug delivery. Pharm. Chem. J. 45, 568–574.
Nogami, H., Nagai, T., Fukuoka, E., Sonobe, T., 1969. Disintegration of the aspirin tablets containing potato starch and microcrystalline cellulose in various concentrations. Chem. Pharm. Bull. 17, 1450–1455.
Obeidat, W.M., Abu Znait, A.a.H., Sallam, A.-S.A., 2008. Novel combination of anionic and cationic polymethacrylate polymers for sustained release tablet preparation. Drug Dev. Ind. Pharm. 34, 650–660.
Olivera, M.E., Manzo, R.H., Alovero, F., Jimenez-Kairuz, A.F., Ramírez-Rigo, M.V., 2017. Polyelectrolyte-drug ionic complexes as nanostructured drug carriers to design solid and liquid oral delivery systems. In: Andronescu, E., Grumezescu, A.M. (Eds.), Nanostructures for Oral Medicine, 1st ed. Elsevier, pp. 365–408.
Palena, M., Manzo, R., Jimenez-Kairuz, A., 2012. Self-organized nanoparticles based on drug-interpolyelectrolyte complexes as drug carriers. J. Nanopart. Res. 14, 1–12.
Palena, M., García, M., Manzo, R., Jimenez-Kairuz, A., 2015. Self-organized drug-interpolyelectrolyte nanocomplexes loaded with anionic drugs. Characterization and in vitro release evaluation. J. Drug Delivery Sci. Technol. 30, 45–53.
Palmeiro-Roldán, R., Fonseca-Berzal, C., Gómez-Barrio, A., Arán, V.J., Escario, J.A., Torrado-Durán, S., Torrado-Santiago, S., 2014. Development of novel benznidazole formulations: physicochemical characterization and in vivo evaluation on parasitemia reduction in Chagas disease. Int. J. Pharm. 472, 110–117.
Pan, X., Chen, M., Han, K., Peng, X., Wen, X., Chen, B., Wang, J., Li, G., Wu, C., 2010. Novel compaction techniques with pellet-containing granules. Eur. J. Pharm. Biopharm. 75, 436–442.
Patra, C.N., Priya, R., Swain, S., Jena, G.K., Panigrahi, K.C., Ghose, D., 2017. Pharmaceutical significance of Eudragit: a review. Futur. J. Pharm. Sci. 3, 33–45.
Peppas, N., 1985. Analysis of Fickian and non-Fickian drug release from polymers. Pharm. Acta Helv. 60, 110.
Pérez, P., Suñé-Negre, J.M., Miñarro, M., Roig, M., Fuster, R., García-Montoya, E., Hernández, C., Ruhí, R., Ticó, J.R., 2006. A new expert systems (SeDeM diagram) for control batch powder formulation and preformulation drug products. Eur. J. Pharm. Biopharm. 64, 351–359.
Prado, H., Matulewicz, M., Bonelli, P., Cukierman, A., 2008. Basic butylated methacrylate copolymer/kappa-carrageenan interpolyelectrolyte complex: preparation, characterization and drug release behaviour. Eur. J. Pharm. Biopharm. 70, 171–178.
Rassi, A.J., Rassi, A., Marin-Neto, J., 2010. Chagas disease. Lancet 375, 1388–1402.
Retsch GmbH, 2017. International Comparison Table for Test Sieves. Table for Standards, Test Sieve Comparison.
de Robertis, S., Bonferoni, M.C., Elviri, L., Sandri, G., Caramella, C., Bettini, R., 2015. Advances in oral controlled drug delivery: the role of drug–polymer and interpolymer non-covalent interactions. Expert Opin. Drug Deliv. 12, 441–453.
Saigal, N., Baboota, S., Ahuja, A., Ali, J., 2009. Multiple-pulse drug delivery systems: setting a new paradigm for infectious disease therapy. Expert Opin. Drug Deliv. 6, 441–452.
Severino, P., de Oliveira, G.G., Ferraz, H.G., Souto, E.B., Santana, M.H., 2012. Preparation of gastro-resistant pellets containing chitosan microspheres for improvement of oral didanosine bioavailability. Chin. J. Pharm. Anal. 2, 188–192.
Siepmann, J., Peppas, N., 2001. Modeling of drug release from delivery systems based on hydroxypropyl methylcellulose (HPMC). Adv. Drug Deliv. Rev. 48, 139–157.
Soares-Sobrinho, J.L., Santos, F.L., Lyra, M.A., Alves, L.D., Rolim, L.A., Lima, A.A., Nunes, L.C., Soares, M.F., Rolim-Neto, P.J., Torres-Labandeira, J.J., 2012. Benznidazole drug delivery by binary and multicomponent inclusion complexes using cyclodextrins and polymers. Carbohydr. Polym. 89, 323–330.
Streck, L., de Araújo, M.M., de Souza, I., Fernandes-Pedrosa, M.F., do Egito, E.S.T., de Oliveira, A.G., da Silva-Júnior, A.A., 2014. Surfactant–cosurfactant interactions and process parameters involved in the formulation of stable and small droplet-sized benznidazole-loaded soybean O/W emulsions. J. Mol. Liq. 196, 178–186.
Takeuchi, H., Thongborisute, J., Matsui, Y., Sugihara, H., Yamamoto, H., Kawashima, Y., 2005. Novel mucoadhesion tests for polymers and polymer-coated particles to design optimal mucoadhesive drug delivery systems. Adv. Drug Deliv. Rev. 57, 1583–1594.
Thünemann, A.F., Müller, M., Dautzenberg, H., Joanny, J.-F., Löwen, H., 2004. Polyelectrolyte complexes. In: Polyelectrolytes with Defined Molecular Architecture II. Springer, pp. 113–171.
U.S. Pharmacopoeial Convention, 2015. United States Pharmacopoeia. 38 The National Formulary and Dispensing Information (33) United States Pharmacopeia Convention Inc., Rockville, Maryland.
Urbina, J., 2010. Specific chemotherapy of Chagas disease: relevance, current limitations and new approaches. Acta Trop. 115, 55–68.
Vila Jato, J., 1997. Tecnología Farmacéutica–Aspectos fundamentales de los sistemas farmacéuticos y operaciones básicas. Editorial Síntesis, Madrid, pp. 75–142.
Wang, J., Somasundaran, P., 2006. Mechanisms of ethyl (hydroxyethyl) cellulose–solid interaction: influence of hydrophobic modification. J. Colloid Interface Sci. 293, 322–332.
World Health Organization, 2015a. Chagas disease. In: Special Programme for Research and Training in Tropical Diseases.
World Health Organization (Ed.), 2015. The International Pharmacopoeia, 5th ed. World Health Organization.